Received: 30 September 2020

DOI: 10.1002/mma.7114

RESEARCH ARTICLE

WILEY

Numerical simulation for time-fractional nonlinear reaction–diffusion system on a uniform and nonuniform time stepping

Waheed K. Zahra[1,2] | **Manal M. Hikal**[1,3] | **Dumitru Baleanu**[4,5,6]

[1]Department of Engineering Physics and Mathematics, Faculty of Engineering, Tanta University, Tanta, Egypt

[2]Department of Mathematics, Institute of Basic and Applied Sciences, Egypt-Japan University of Science and Technology (E-JUST), New Borg El-Arab City, Egypt

[3]Department of Basic Sciences, Higher Institute of Engineering and Technology Kafrelsheikh, Kafr Al Sheikh, Egypt

[4]Department of Mathematics, Cankaya University, Ankara, Turkey

[5]Institute of Space Sciences, Magurele-Bucharest, Romania

[6]Department of Medical Research, China Medical University Hospital, Taichung City, China

Correspondence
W. K. Zahra, Department of Engineering Physics and Mathematics, Faculty of Engineering, Tanta University, Tanta 31521, Egypt.
Email: waheed_zahra@yahoo.com; waheed.zahra@ejust.edu.eg; wzahra@f-eng.tanta.edu.eg

In this article, two nonstandard high-order schemes on a uniform and nonuniform time stepping combined with the multi-parameter exponential fitting technique (MPEF) have been developed to solve the time-fractional nonlinear reaction–diffusion system. The first method based on the MPEF combined with the 3-weighted shifted-Grünwald–Letnikov approximation with uniform time stepping, this scheme leads to a numerical solution that suffers from the singularity near $t = 0$. In order to frustrate this singularity, a nonstandard higher-order L1-approximation for a nonuniform time-stepping scheme is developed. The developed scheme's convergence and unconditionally stability analysis have been verified. Numerical results effectively validate the theoretical aspects.

KEYWORDS

Caputo fractional derivative, convergence analysis, exponential fitting, nonuniform time stepping, stability

JEL CLASSIFICATION

65M12; 65N12; 65L70

1 | INTRODUCTION

The time-fractional nonlinear reaction–diffusion system has the following general form:

$$D_t^\alpha u = K_1 D_x^2 u - \alpha_0 + \alpha_1 u + \alpha_2 v + \alpha_3 u^2 + \alpha_4 v^2 + \alpha_5 uv + \alpha_6 u^2 v + \alpha_7 uv^2,\ 0 < \alpha \le 1, \tag{1a}$$

$$D_t^\alpha v = K_2 D_x^2 v - \beta_0 + \beta_1 u + \beta_2 v + \beta_3 u^2 + \beta_4 v^2 + \beta_5 uv + \beta_6 u^2 v + \beta_7 uv^2, \tag{1b}$$

subject to the initial conditions

$$u(x,0) = p_1(x),\ v(x,0) = p_2(x),\quad x_a \le x \le x_b, \tag{2}$$

and the boundary conditions

$$u(x_a,t)-h_1(t)=u(x_b,t)-h_2(t)=0,\quad 0\le t\le T, \tag{3a}$$

$$v(x_a,t)-g_1(t)=v(x_b,t)-g_2(t)=0, \tag{3b}$$

where $p_i(x)$, $h_i(t)$, $g_i(t)$, $i=1,2$ are smooth continuous functions, α_i, β_i, $i=0,1,...,7$ are constants, and the operator D_t^α represents the Caputo fractional derivative.

Nonlinear reaction–diffusion equations (NRDEs) are a mathematical tool that describes many phenomena in engineering and science. Due to the existence of the reaction and diffusion terms, NRDSs can tackle complicated behaviors such as the Gray–Scott model, Belousov–Zhabotinskii reaction systems, Gierer–Meinhardt model, Lengyel–Epstein system, wave optics, and spread of infectious diseases; see Onarcan et al.[1]

Nowadays, the non-integer-order derivative plays a vital role in modeling many processes in physics, engineering, and science such as optimal control problems,[2] heat transfer model,[3,4] convection–diffusion reaction equations,[5] quantum mechanics,[6–8] fractional predator–prey biological model,[9] fractional tumor-immune models,[10,11] and the reference therein. The fractional nonlinear reaction–diffusion equations (FNRDEs) appear in many applications such as gas transport model,[12] gas dynamics system,[13] the Lotka–Volterra type,[14,15] fractional telegraph equation,[16] chaotic dynamical systems,[17] diffusion with reaction terms,[18,19] Gray–Scott model,[20,21] reaction–diffusion system arising in biology,[22] Belousov–Zhabotinskii reaction systems,[23] Gierer–Meinhardt model,[24] Lengyel–Epstein system,[25] and dynamics of coronavirus (2019-nCov).[26] Also, the new fractional derivatives that have nonsingular kernel are given in Kumar et al.,[27,28] fractional Navier–Stokes equation,[29] Boussinesq–Burger's equation,[30] and the nonlinear Kaup–Kupershmidt equation.[31]

For the numerical methods dealing with the non-integer-order differential equations, many authors have developed numerical methods such as exponentially fitted methods and[32–35] high-order difference schemes.[36,37] On the other hand, some numerical methods have been developed for nonuniform mesh such as the L1-approximation scheme,[38,39] error analysis of time stepping with nonsmooth data,[40] and the finite difference with nonuniform time stepping (NUTS).[41] Recently, previous studies[42–46] proposed a finite difference method with nonuniform time steps to solve diffusion, advection, and Allen–Cahn equations.

In this paper, we will introduce a new nonstandard higher-order L1-approximation combined with the multiparameter of exponentially fitted (MPEF) methods on NUTS to find the approximate solution of a system of time-fractional nonlinear diffusion. The main advantage of the suggested technique is to annihilate and overcome the difficulties that arise due to the singularity behavior near $t=0$. Also, MPEF enables us to get the best μ-parameter to promote high-order accuracy. Finally, we will show that the suggested technique is superior to the uniform time-stepping schemes.

The article is organized as follows: Temporal discretization has been developed in Section 2, while the MPEF method is introduced in Section 3. In Section 4, we present the numerical approximation for both uniform and NUTS. Section 5 is devoted to stability and convergence analysis, and Section 6 deals with the numerical examples that validate the theoretical aspects. Finally, the conclusions are summarized in Section 7.

2 | TEMPORAL DISCRETIZATION

2.1 | Basic definitions

The following basic definitions and properties in the theory of fractional calculus need to be introduced before proceeding; see previous studies.[47–49]

Definition 1. The Caputo fractional operator is

$${}^{C}D_t^\alpha\phi(x,t)=\frac{1}{\Gamma(1-\alpha)}\int_0^t(t-\zeta)^{-\alpha}D_\zeta\phi(x,\zeta)d\zeta,\quad 0<\alpha\le 1, \tag{4}$$

where $\Gamma(.)$ denotes Gamma function.

Definition 2. The Riemann–Liouville (RL) derivative is

$$^{RL}D_t^{\alpha}\phi(x,t)=\frac{1}{\Gamma(1-\alpha)}\frac{\partial}{\partial t}\int_0^t(t-\zeta)^{-\alpha}\phi(x,\zeta)d\zeta,\quad 0<\alpha\leq 1. \tag{5}$$

The relation between the Caputo and RL fractional derivatives is defined as follows.[50,51]

$$^{C}D_t^{\alpha}\phi(x,t)=\,^{RL}D_t^{\alpha}[\phi(x,t)-\phi(x,0)]. \tag{6}$$

Definition 3. The shifted-Grünwald-Letnikov (SGL) derivative is

$$D_{t,s}^{\alpha}\phi(x,t)=\lim_{\tau\to 0}\frac{1}{\tau^{\alpha}}\sum\nolimits_{k=0}^{\left[\frac{t}{\tau}\right]+s}g_k^{\alpha}\phi(x,t-(k-s)\tau), \tag{7}$$

where s is a constant and the coefficients g_k^{α} can be evaluated as

$$g_0^{\alpha}=1,\ \ g_k^{\alpha}=\left(1-\frac{\alpha+1}{k}\right)g_{k-1}^{\alpha},\ k=1,2,3,.... \tag{8}$$

If $s=0$, we get the GL formula,[8] and the GL coefficients satisfy[52]

$$g_0^{\alpha}=1,\ g_1^{\alpha}=-\alpha\leq 0,\ g_2^{\alpha}\leq g_3^{\alpha}\leq g_4^{\alpha}\leq ...\leq 0,\ \sum\nolimits_{k=0}^{\infty}g_k^{\alpha}=0,\ \sum\nolimits_{k=0}^{n}g_k^{\alpha}\geq 0,\ n\geq 1. \tag{9}$$

Definition 4. The Caputo–Fabrizio (CF) derivative is

$$^{CF}D_t^{\alpha}\phi(x,t)=\frac{M(\alpha)}{1-\alpha}\int_0^t D_{\zeta}\phi(x,\zeta)\exp[-\delta(t-\zeta)]d\zeta,\delta=\frac{\alpha}{1-\alpha},M(0)=M(1)=1,M(\alpha)=\frac{2}{2-\alpha}. \tag{10}$$

Definition 5. The Atangana–Baleanu (AB) derivative is

$$^{AB}D_t^{\alpha}\phi(x,t)=\frac{M(\alpha)}{1-\alpha}\int_0^t D_{\zeta}\phi(x,\zeta)E_{\alpha}[-\delta(t-\zeta)^{\alpha}]d\zeta,E_{\alpha}(-t)^{\alpha}=\sum\nolimits_{k=0}^{\infty}\frac{(-t)^{\alpha k}}{\Gamma(\alpha k+1)}. \tag{11}$$

Definition 6. The conformable fractional derivative (CFD) is

$$^{CFD}D_t^{\alpha}\phi(x,t)=\lim_{\varepsilon\to 0}\frac{1}{\varepsilon}\left(\phi\left(x,t+\varepsilon\, t^{1-\alpha}\right)-\phi(x,t)\right), \tag{12}$$

for all $t>0$. If ϕ is α-differentiable in some $(0,a)$, $a>0$, and $\lim_{t\to 0^+}\phi^{(\alpha)}(x,t)$ exists, then

$$^{CFD}D_t^{\alpha}\phi(x,0)=\lim_{t\to 0^+}\,^{CFD}D_t^{\alpha}\phi(x,t). \tag{13}$$

Additionally, if the CFD of ϕ of order α exists, then it can be said that ϕ is α-differentiable. In case ϕ is ordinary differentiable, the CFD is connected with the ordinary derivative, for $t>0$, by

$$^{CFD}D_t^{\alpha}\phi(t)=t^{1-\alpha}\phi'(t), \tag{14}$$

where the ordinary derivative of ϕ is denoted by $\phi'(t)$ at the point t. For more details about other fractional operators, we may refer to the reference.[47]

2.2 | Uniform temporal discretization

Let the interval $[0,T]$ be dived into N equal subintervals with $0 = t_0 < t_1 < t_2 < ... < t_N = T$, where $t_j = t_0 + j\tau, \tau = \frac{T}{N}, j = 1,2,...,N$.

Using the SGL derivative given by Equation 7, we can approximate the RL derivative using the SGL derivative.[52,53]

$$^{RL}D^{\alpha}_{t,s}\phi(x,t) \cong \frac{1}{\tau^{\alpha}}\sum\nolimits_{k=0}^{j-s} g^{\alpha}_{k}\phi\left(x,t_{j-(k-s)}\right). \tag{15}$$

Lemma 2.1. Let $\phi \in \mathcal{H}^{3+\alpha}(\mathbb{R})$ and $\phi^{(e+\alpha)} \in L^1(\mathbb{R})$, $e = 1,2,3$, the 3-WSGL approximation for $0 < \alpha \leq 1$ is; see Gao et al.[52]

$$^{RL}D^{\alpha}_{t}\phi(x,t) = \tau^{-\alpha}\sum\nolimits_{k=0}^{\infty} w^{\alpha}_{k}\phi\left(x,t_{j-k+1}\right) + O\left(\tau^{3}\right), \tag{16}$$

where

$$w^{\alpha}_{0} = \varphi_1 g^{\alpha}_{0}; w^{\alpha}_{1} = \varphi_1 g^{\alpha}_{1} + \varphi_2 g^{\alpha}_{0};\ w^{\alpha}_{k} = \varphi_1 g^{\alpha}_{k} + \varphi_2 g^{\alpha}_{k-1} + \varphi_3 g^{\alpha}_{k-2}, k \geq 2. \tag{17}$$

and $\varphi_1 = \frac{5\alpha + 3\alpha^2}{24},\ \varphi_2 = 1 + \frac{\alpha - 3\alpha^2}{12},\ \varphi_3 = \frac{-7\alpha + 3\alpha^2}{24}$.

Also, using the nonstandard finite difference, we get the new approximation as

$$^{RL}D^{\alpha}_{t}\phi(x,t) \cong (\psi(\tau))^{-\alpha}\sum\nolimits_{k=0}^{j+1} w^{\alpha}_{k}\phi\left(x,t_{j-k+1}\right), \tag{18}$$

where τ is replaced by the $\psi(\tau) = \tau + O(\tau^2)$ and $\psi(\tau)$ be chosen as τ,sin τ; see previous studies.[54,55]

2.3 | Nonuniform temporal discretization

Using the same number of subintervals as in Section 2.1, we have

$$t_j = T\left(\frac{j}{N}\right)^{r}, r > 0, \tau_j = t_j - t_{j-1}, 1 \leq j \leq N.$$

We will see that there is a singularity near $t_0 = 0$; to overcome this situation, we need to use NUTS. The L1 formula for approximating the Caputo fractional derivative is given as in the following Lemma:

Lemma 2.2. The L1-approximation formula for the Caputo fractional derivative is given by[42]

$$^{C}D^{\alpha}_{t}\phi\left(x,t_j\right) = \sum\nolimits_{k=1}^{j} a^{j}_{k}\left(\phi(x,t_k) - \phi(x,t_{k-1})\right),\ 1 \leq k \leq j; \tag{19}$$

we may write $a^{j}_{k} = \frac{1}{\tau_k \Gamma(2-\alpha)}\left[\left(t_j - t_{k-1}\right)^{1-\alpha} - \left(t_j - t_k\right)^{1-\alpha}\right]$, and the coefficients $\left\{a^{j}_{k}\right\}_{1}^{j}$ satisfy

$$0 < a^{j}_{1} < a^{j}_{2} < ... < a^{j}_{k-1} < a^{j}_{k} < ... < a^{j}_{j-1} < a^{j}_{j}.$$

Lemma 2.3. The nonstandard higher-order L1-approximation formula for the Caputo fractional derivative is given by

$$ {}^{C}D_t^{\alpha}\phi(x,t_j)=\sum_{k=1}^{j}c_k^j(\phi(x,t_k)-\phi(x,t_{k-1})),1\le k\le j, \tag{20}$$

where $c_1^j=a_1^j$, and

$$ c_k^j=\begin{cases} a_1^j-\dfrac{1}{\Gamma(2-\alpha)}\dfrac{1}{\psi(\tau_1)(\psi(\tau_1)+\psi(\tau_2))}b_2^j, & k=2,\\ a_k^j-\dfrac{1}{\Gamma(2-\alpha)}\left(\dfrac{1}{\psi(\tau_k)(\psi(\tau_{k-1})+\psi(\tau_k))}b_k^j-\dfrac{1}{\psi(\tau_k)(\psi(\tau_k)+\psi(\tau_{k+1}))}b_{k+1}^j\right), & 2\le k\le j-1,\\ a_j^j-\dfrac{1}{\Gamma(2-\alpha)}\dfrac{1}{\psi(\tau_j)\left(\psi(\tau_{j-1})+\psi(\tau_j)\right)}b_j^j, & k=j, \end{cases} \tag{21}$$

and $b_k^j=\frac{2}{(2-\alpha)}\left[(t_j-t_{k-1})^{2-\alpha}-(t_j-t_k)^{2-\alpha}\right]-\psi(\tau_k)\left[(t_j-t_{k-1})^{1-\alpha}-(t_j-t_k)^{1-\alpha}\right]$.

Proof. Follow the same procedure as in Soori and Aminataei.[42]

Lemma 2.4. For $0<\alpha\le 1$, and $\psi(\tau_k)=\tau_k$, the coefficients $\left\{c_k^j\right\}_1^j$ satisfy[42]

$$ \mathrm{c_k^j}>0,\mathrm{k}\neq 1,\mathrm{j}\neq 2,\ c_1^j<c_2^j<\ldots<c_{k-1}^j<c_k^j<\ldots<c_{j-1}^j<c_j^j. \tag{22}$$

3 | THE MPEF METHOD

To introduce the MPEF methods, we consider the following:

$$ u_{xx}=f(x,u). \tag{23}$$

For details of the EF approach, we refer to previous studies.[32,34,35,56–59]

Let $x_i=x_a+ih,\ h=\frac{x_b-x_a}{m},i=0,1,\ldots,\mathrm{m},\ m\ge 3$. To get the approximate solution of the problem 23, we apply the following EF scheme:

$$ u_{i-1}+a_0u_i+u_{i+1}=h^2(b_1M_{i-1}+b_0M_i+b_1M_{i+1}), \tag{24}$$

where u_i is the approximate value of the exact solution $u(x_i)$ and $M_i=u_{xx}(x_i)$. To evaluate the constants a_0, b_i, $i=0,1$, we need to define the following operator:

$$ \int[h,a]u(x):=u(x-h)+a_0u(x)+u(x+h)-h^2(b_1u''(x-h)+b_0u''(x)+b_1u''(x+h)), \tag{25}$$

with the fitting space

$$ \varrho_{K,P}=\left\{1,x,\ x^2,\ldots,x^K\right\}\cup\left\{exp(\pm\mu_0x),xexp(\pm\mu_1x),x^2exp(\pm\mu_2x),\ldots,x^Pexp(\pm\mu_Px)\right\}, \tag{26}$$

where $K+2P=N-3$, μ_q, $q=0,\ldots,P$ are either real or complex.

A class of MPEF procedures to solve 23 is given as follows.

Lemma 3.1. The MPEF approach (24–26) develops $\mathbf{S_1}$–$\mathbf{S_4}$ methods as

$$\mathbf{S1}: P=-1: \quad (a_0,b_0,b_1)=\left(-2,\frac{5}{6},\frac{1}{12}\right), lte_i=\frac{-h^6}{240}D_x^6u_i+O\left(h^8\right).$$

$$\mathbf{S2}: P=0: \quad (a_0,b_0,b_1)=\left(-2,\frac{-2\xi_0+2+\xi_0Z_0}{Z_0(\xi_0-1)},\frac{-Z_0-2\xi_0+2}{2Z_0(\xi_0-1)}\right), lte_i=h^6\left(D_x^6u_i-\mu_0^2D_x^4u_i\right)+O\left(h^8\right).$$

$$\mathbf{S3}: P=1: (a_0,b_0,b_1)=\left(-2,-2\frac{\xi_0(\xi_1-1)Z_0+\xi_1(1-\xi_0)Z_1}{Z_0Z_1(\xi_1-\xi_0)},\frac{(\xi_1-1)Z_0+(1-\xi_0)Z_1}{Z_0Z_1(\xi_1-\xi_0)}\right), lte_i=h^6\left(D_x^6u_i-\left(\mu_0^2+\mu_1^2\right)D_x^4u_i+\mu_0^2\mu_1^2D_x^2u_i\right)+O\left(h^8\right).$$

$$\mathbf{S4}: P=2: a_0=-2\frac{-\xi_0(\xi_1-\xi_2)Z_0Z_1+\xi_2(\xi_1-\xi_0)Z_0Z_1+\xi_1(\xi_0-\xi_2)Z_0Z_2}{Z_1Z_2(\xi_2-\xi_1)+Z_0Z_1(\xi_1-\xi_0)+Z_0Z_2(\xi_0-\xi_2)}, b_0=-2\frac{-\xi_1(\xi_0-\xi_2)Z_1-\xi_2(\xi_1-\xi_0)Z_2+\xi_0(\xi_1-\xi_2)Z_0}{Z_1Z_2(\xi_2-\xi_1)+Z_0Z_1(\xi_1-\xi_0)+Z_0Z_2(\xi_0-\xi_2)},$$

$$b_1=\frac{(\xi_2-\xi_0)Z_1-(\xi_1-\xi_0)Z_2+(\xi_1-\xi_2)Z_0}{Z_1Z_2(\xi_2-\xi_1)+Z_0Z_1(\xi_1-\xi_0)+Z_0Z_2(\xi_0-\xi_2)},$$

$$lte_i=h^6\left(D_x^6u_i-\left(\mu_0^2+\mu_1^2+\mu_2^2\right)D_x^4u_i+\left(\mu_0^2\mu_1^2+\mu_0^2\mu_2^2+\mu_1^2\mu_2^2\right)D_x^2u_i-\mu_0^2\mu_1^2\mu_2^2u_i\right)+O\left(h^8\right),$$

where $\bar{\xi}_q=\bar{\xi}\left(Z_q\right)$ and $\bar{\bar{\xi}}_q=\bar{\bar{\xi}}\left(Z_q\right)$ are in Ixaru and Vanden Berghe[56] and defined as

$$\bar{\xi}(Z)=\cos\left(I\sqrt{Z}\right), \bar{\bar{\xi}}(Z)=\begin{cases}\dfrac{Sin\,I\sqrt{Z}}{I\sqrt{Z}}, & Z\neq 0\\ 1, & Z=0,\end{cases}\ Z_q=\left(\mu_q h\right)^2.$$

4 | NUMERICAL APPROXIMATION

Now, we apply MPEF introduced in 23 to solve the reaction–diffusion system (1a–3b) at the point (x_i, t_j). Then the MPEF scheme for the problem 1a has the form:

$$\left(u_{i-1}^j+\mathfrak{a}_0\,u_i^j+u_{i+1}^j\right)=h^2\left(b_1\,M_{i-1}^j+b_0\,M_i^j+b_1\,M_{i+1}^j\right), \tag{27}$$

where $M_i^j=D_x^2u\left(x_i,t_j\right)$, and for two different time levels j and j+1, one has

$$\left(u_{i-1}^j+\mathfrak{a}_0\,u_i^j+u_{i+1}^j\right)+\left(u_{i-1}^{j+1}+\mathfrak{a}_0\,u_i^{j+1}+u_{i+1}^{j+1}\right)=h^2\left[b_1\left(\mathrm{M}_{i-1}^j+\mathrm{M}_{i-1}^{j+1}\right)+b_0\left(\mathrm{M}_i^j+\mathrm{M}_i^{j+1}\right)+b_1\left(\mathrm{M}_{i+1}^j+\mathrm{M}_{i+1}^{j+1}\right)\right]. \tag{28}$$

Let

$$f_1(x,t,u,v)=\alpha_0+\alpha_1u+\alpha_2v+\alpha_3u^2+\alpha_4v^2+\alpha_5uv+\alpha_6u^2v+\alpha_7uv^2, \tag{29}$$

$$f_2(x,t,u,v)=\beta_0+\beta_1u+\beta_2v+\beta_3u^2+\beta_4v^2+\beta_5uv+\beta_6u^2v+\beta_7uv^2.$$

Then applying the Crank–Nicolson scheme for the system (1a,1b), we have

$${}^{C}D_t^{\alpha}u\left(x_i,t_j\right)=\frac{1}{2}\left[K_1\left(\mathrm{M}_i^j+\mathrm{M}_i^{j+1}\right)-f_{1i}^{\,j}-f_{1i}^{\,j+1}\right], \tag{30a}$$

$$ {}^{C}D_t^{\alpha} v(x_i,t_j) = \frac{1}{2}\left[K_2\left(\mathrm{L}_i^j + \mathrm{L}_i^{j+1}\right) - f_{2i}^{\ j} - f_{2i}^{\ j+1}\right], \tag{30b} $$

where $L_i^j = D_x^2 v(x_i,t_j), f_{1i}^{\ j} = f_1\left(x_i,t_j,u_i^j,v_i^j\right)$ and $f_{2i}^{\ j} = f_2\left(x_i,t_j,u_i^j,v_i^j\right)$.

4.1 | Numerical approximation via uniform time stepping

Using the approximation given by Equation 18, along with Equation 6 in Equations 28 and 29, we get the following:

$$ \begin{aligned} u_{i-1}^{j+1} + \mathfrak{a}_0\, u_i^{j+1} + u_{i+1}^{j+1} + u_{i-1}^{j} + \mathfrak{a}_0\, u_i^{j} + u_{i+1}^{j} = \frac{h^2}{k}\Bigg[& \Bigg(2\,b_1(\psi(\tau))^{-\alpha} \sum_{k=0}^{j+1} w_k^{\alpha} u_{i-1}^{j-k+1} - \frac{2b_1 p_{1i-1}}{t_j^{\alpha}\Gamma(1-\alpha)} \\ & + 2b_0(\psi(\tau))^{-\alpha} \sum_{k=0}^{j+1} w_k^{\alpha} u_i^{j-k+1} - \frac{2b_0 p_{1i}}{t_j^{\alpha}\Gamma(1-\alpha)} + 2b_1(\psi(\tau))^{-\alpha} \sum_{k=0}^{j+1} w_k^{\alpha} u_{i+1}^{j-k+1} - \frac{2b_1 p_{1i+1}}{t_j^{\alpha}\Gamma(1-\alpha)} \Bigg) \\ & + \left(b_1 f_{1i-1}^{\ j+1} + b_0 f_{1i}^{\ j+1} + b_1 f_{1i+1}^{\ j+1} \right) + \left(b_1 f_{1i-1}^{\ j} + b_0 f_{1i}^{\ j} + b_1 f_{1i+1}^{\ j} \right) \Bigg], \end{aligned} \tag{31} $$

and

$$ \begin{aligned} v_{i-1}^{j+1} + \mathfrak{a}_0\, v_i^{j+1} + v_{i+1}^{j+1} + v_{i-1}^{j} + \mathfrak{a}_0\, v_i^{j} + v_{i+1}^{j} = \frac{h^2}{k}\Bigg[& \Bigg(2\,b_1(\psi(\tau))^{-\alpha} \sum_{k=0}^{j+1} w_k^{\alpha} v_{i-1}^{j-k+1} - \frac{2b_1 p_{2i-1}}{t_j^{\alpha}\Gamma(1-\alpha)} \\ & + 2b_0(\psi(\tau))^{-\alpha} \sum_{k=0}^{j+1} w_k^{\alpha} v_i^{j-k+1} - \frac{2b_0 p_{2i}}{t_j^{\alpha}\Gamma(1-\alpha)} + 2b_1(\psi(\tau))^{-\alpha} \sum_{k=0}^{j+1} w_k^{\alpha} v_{i+1}^{j-k+1} - \frac{2b_1 p_{2i+1}}{t_j^{\alpha}\Gamma(1-\alpha)} \Bigg) \\ & + \left(b_1 f_{2i-1}^{\ j+1} + b_0 f_{2i}^{\ j+1} + b_1 f_{2i+1}^{\ j+1} \right) + \left(b_1 f_{2i-1}^{\ j} + b_0 f_{2i}^{\ j} + b_1 f_{2i+1}^{\ j} \right) \Bigg]. \end{aligned} \tag{32} $$

Let $U^j = \left(u_i^j\right)$ and $V^j = \left(v_i^j\right)$ be the approximate solutions and $\boldsymbol{u}^j = (u(x_i,t_j))$ and $\boldsymbol{v}^j = (v(x_i,t_j))$ be the exact solutions. Also, the local truncation errors are $\boldsymbol{T}^j = \left(T_i^j\right)$. Then the matrix equations of the above discrete system are

$$ \left(A - \frac{2h^2 w_0^{\alpha}}{k_1(\psi(\tau))^{\alpha}} B\right)\boldsymbol{u}^{j+1} - \frac{h^2}{k_1} B\boldsymbol{f_1}^{j+1} = -A\boldsymbol{u}^j + \frac{h^2}{2k_1(\psi(\tau))^{\alpha}} B \sum_{k=1}^{j+1} w_k^{\alpha} \boldsymbol{u}^{j-k+1} + \frac{h^2}{k} B\boldsymbol{f_1}^j - \frac{2}{t_j^{\alpha}\Gamma(1-\alpha)} B P_1^0 + C^j + \boldsymbol{T}^j,\ j = 0,1,2,\ldots,n, \tag{33} $$

and

$$ \left(A - \frac{2h^2 w_0^{\alpha}}{k_2(\psi(\tau))^{\alpha}} B\right)\boldsymbol{v}^{j+1} - \frac{h^2}{k_1} B\boldsymbol{f_2}^{j+1} = -A\boldsymbol{v}^j + \frac{h^2}{2k_2(\psi(\tau))^{\alpha}} B \sum_{k=1}^{j+1} w_k^{\alpha} \boldsymbol{v}^{j-k+1} + \frac{h^2}{k} B\boldsymbol{f_2}^j - \frac{2}{t_j^{\alpha}\Gamma(1-\alpha)} B P_2^0 D^j + \boldsymbol{T}^j,\ j = 0,1,2,\ldots,n, \tag{34} $$

where $A = Tri(a_0, 1)$ and $B = Tri(b_0, b_1)$ are tridiagonal matrices of order $m-1$, where

$$ Tri(a,b) = \begin{cases} a, & i = j \\ b, & |i-l| = 1 \\ 0, & \text{otherwise.} \end{cases} \quad ,i,l = 1,2,3,\ldots,m-1, $$

$$C^j = \begin{bmatrix} -h_1^j - h_1^{j+1} + \frac{2b_1h^2}{k_1(\psi(\tau))^\alpha}\sum_{k=0}^{j+1} w_k^\alpha h_1^{j-k+1} - \frac{2b_1h^2p_{10}}{k_1t_j^\alpha\Gamma(1-\alpha)} + \frac{b_1h^2}{k_1}\left(f_{10}^{\ j} + f_{10}^{\ j+1}\right) \\ 0 \\ \vdots \\ 0 \\ -h_2^j - h_2^{j+1} + \frac{2b_1h^2}{k_1(\psi(\tau))^\alpha}\sum_{k=0}^{j+1} w_k^\alpha h_2^{j-k+1} - \frac{2b_1h^2p_{1m}}{k_1t_j^\alpha\Gamma(1-\alpha)} + \frac{b_1h^2}{k_1}\left(f_{1m}^{\ j} + f_{1m}^{\ j+1}\right) \end{bmatrix}, \text{and}$$

$$D^j = \begin{bmatrix} -g_1^j - g_1^{j+1} + \frac{2b_1h^2}{k_1(\psi(\tau))^\alpha}\sum_{k=0}^{j+1} w_k^\alpha g_1^{j-k+1} - \frac{2b_1h^2p_{20}}{k_1t_j^\alpha\Gamma(1-\alpha)} + \frac{b_1h^2}{k_1}\left(f_{20}^{\ j} + f_{20}^{\ j+1}\right) \\ 0 \\ \vdots \\ 0 \\ -g_2^j - g_2^{j+1} + \frac{2b_1h^2}{k_1(\psi(\tau))^\alpha}\sum_{k=0}^{j+1} w_k^\alpha g_2^{j-k+1} - \frac{2b_1h^2p_{2m}}{k_1t_j^\alpha\Gamma(1-\alpha)} + \frac{b_1h^2}{k_1}\left(f_{2m}^{\ j} + f_{2m}^{\ j+1}\right) \end{bmatrix}.$$

The nonlinear functions $f_i(x,t,u,v), i = 1,2$ satisfy the Lipschitz condition.

$$|f_1(x,t,u,v) - f_1(x,t,w,v)| \le L_u|u-w|, |f_2(x,t,u,v) - f_2(x,t,u,z)| \le L_v|v-z|, 0 < L_u, L_v < 1, \tag{35}$$

where L_u, L_v are called a Lipschitz constant.

We can linearize the nonlinear terms with aid of the study given in previous studies[1,60,61] as

$$\begin{aligned} \left(u_i^{j+1}\right)^2 &= 2u_i^j u_i^{j+1} - \left(u_i^j\right)^2, \quad \left(v_i^{j+1}\right)^2 = 2v_i^j v_i^{j+1} - \left(v_i^j\right)^2, u_i^{j+1}v_i^{j+1} = u_i^{j+1}v_i^j + u_i^j v_i^{j+1} - u_i^j v_i^j, \ \left(u_i^{j+1}\right)^2 v_i^{j+1} = 2u_i^{j+1}u_i^j v_i^j \\ &+ \left(u_i^j\right)^2 v_i^{j+1} - 2\left(u_i^j\right)^2 v_i^j, \left(v_i^{j+1}\right)^2 u_i^{j+1} = 2u_i^j u_i^{j+1} v_i^j + \left(v_i^j\right)^2 u_i^{j+1} - 2\left(v_i^j\right)^2 u_i^j. \end{aligned} \tag{36}$$

Then, we have

$$f_{1i}^{\ j} + f_{1i}^{\ j+1} = G_{1i}^j u_i^{j+1} + R_{1i}^j v_i^{j+1} + S_{1i}^j, \quad f_{2i}^{\ j} + f_{2i}^{\ j+1} = G_{2i}^j u_i^{j+1} + R_{2i}^j v_i^{j+1} + S_{2i}^j, \tag{37}$$

where

$$\begin{aligned} G_{1i}^j &= \alpha_1 u_i^{j+1} + 2\alpha_3 u_i^j + \alpha_5 v_i^j + 2\alpha_6 u_i^j v_i^j + \alpha_7\left(v_i^j\right)^2, \\ R_{1i}^j &= \alpha_2 + 2\alpha_4 v_i^j + \alpha_5 u_i^j + \alpha_6\left(u_i^j\right)^2 + 2\alpha_7 u_i^j v_i^j, \\ S_{1i}^j &= 2\,\alpha_0 + \alpha_1 u_i^j + \alpha_2 v_i^j - \alpha_6\left(u_i^j\right)^2 v_i^j - \alpha_7 u_i^j\left(v_i^j\right)^2, \end{aligned} \tag{38}$$

$$G_{2_i}^j = \beta_1 u_i^{j+1} + 2\beta_3 u_i^j + \beta_5 v_i^j + 2\beta_6 u_i^j v_i^j + \beta_7 \left(v_i^j\right)^2, \tag{39}$$

$$R_{1_i}^j = \beta_2 + 2\beta_4 v_i^j + \beta_5 u_i^j + \beta_6 \left(u_i^j\right)^2 + 2\beta_7 u_i^j v_i^j,$$

$$S_{1_i}^j = 2\beta_0 + \beta_1 u_i^j + \beta_2 v_i^j - \beta_6 \left(u_i^j\right)^2 v_i^j - \beta_7 u_i^j \left(v_i^j\right)^2.$$

Insert 36 into 31 and 32, we have the linear algebraic system

$$A_1 U^{j+1} - B_1 V^{j+1} = C_1, \tag{40a}$$

$$-A_2 U^{j+1} + B_2 V^{j+1} = C_2, \tag{40b}$$

with the matrices

$$A_1 = A - \frac{2h^2 w_0^\alpha}{k_1 (\psi(\tau))^\alpha} B - \frac{2h^2}{k_1} (BG_1)^j, B_1 = \frac{h^2}{k_1} (BR_1)^j, \quad A_2 = \frac{h^2}{k_2} (BG_2)^j,$$

$$B_2 = A - \frac{2h^2 w_0^\alpha}{k_2 (\psi(\tau))^\alpha} B - \frac{2h^2}{k_2} (BR_2)^j,$$

$$C_1 = \frac{2h^2}{k_1 (\psi(\tau))^\alpha} B \sum_{k=1}^{j+1} w_k^\alpha U^{j-k+1} - AU^j - \frac{2h^2}{t_j^\alpha k_1 \Gamma(1-\alpha)} BP_1 + \frac{h^2}{k_1} (BS_1)^j + cd,$$

$$C_2 = \frac{2h^2}{k_2 (\psi(\tau))^\alpha} B \sum_{k=1}^{j+1} w_k^\alpha V^{j-k+1} - AV^j - \frac{2h^2}{t_j^\alpha k_1 \Gamma(1-\alpha)} BP_2 + \frac{h^2}{k_2} (BS_2)^j + dd,$$

$$(BG_1)^j = Tri\left(\left(b_{0l}^G\right)^j, \left(b_{1l}^G\right)^j\right), (BR_1)^j = Tri\left(\left(b_{0l}^R\right)^j, \left(b_{1l}^R\right)^j\right), (BS_1)^j = Tri\left(\left(b_{0l}^S\right)^j, \left(b_{1l}^S\right)^j\right), l = 1, 2,$$

$$Tri\left(\left(b_{0l}^X\right)^j, \left(b_{1l}^X\right)^j\right) = \begin{cases} b_0 (X_l)_i^j, & i = k, \\ b_1 (X_l)_{i-1}^j, & i - k = 1, \\ b_1 (X_l)_{i+1}^j, & i - k = -1, \\ 0, & otherwise, \end{cases} \quad X_l \in \{G_i, R_i, S_i\}, l = 1, 2, \text{and } i, k = 1, 2, ..., m-1,$$

$$cd = \begin{bmatrix} -h_1^j - h_1^{j+1} + \frac{2b_1 h^2}{k_1 (\psi(\tau))^\alpha} \sum_{k=0}^{j+1} w_k^\alpha h_1^{j-k+1} - \frac{2h^2 b_1 p_{10}}{k_1 t_j^\alpha \Gamma(1-\alpha)} + \frac{b_1 h^2}{k_1} \left((G_1)_0^j h_1^{j+1} + (R_1)_0^j v_0^{j+1} + (S_1)_0^j\right) \\ 0 \\ \vdots \\ 0 \\ -h_2^j - h_2^{j+1} + \frac{2b_1 h^2}{k_1 (\psi(\tau))^\alpha} \sum_{k=0}^{j+1} w_k^\alpha h_2^{j-k+1} - \frac{2h^2 b_1 p_{1m}}{k_1 t_j^\alpha \Gamma(1-\alpha)} + \frac{b_1 h^2}{k_1} \left((G_1)_m^j h_1^{j+1} + (R_1)_m^j v_m^{j+1} + (S_1)_m^j\right) \end{bmatrix}, \text{and}$$

$$dd=\begin{bmatrix} -g_1^j-g_1^{j+1}+\frac{2b_1h^2}{k_2(\psi(\tau))^\alpha}\sum_{k=0}^{j+1}w_k^\alpha g_1^{j-k+1}-\frac{2h^2b_1p_{20}}{k_1t_j^\alpha\Gamma(1-\alpha)}+\frac{b_1h^2}{k_2}\left((G_2)_0^j\,h_1^{j+1}+(R_2)_0^j\,v_0^{j+1}+(S_2)_0^j\right)\\ 0\\ \vdots\\ 0\\ -g_2^j-g_2^{j+1}+\frac{2b_1h^2}{k_2(\psi(\tau))^\alpha}\sum_{k=0}^{j+1}w_k^\alpha g_2^{j-k+1}-\frac{2h^2b_1p_{2m}}{k_1t_j^\alpha\Gamma(1-\alpha)}+\frac{b_1h^2}{k_1}\left((G_2)_m^j\,h_1^{j+1}+(R_2)_m^j\,v_m^{j+1}+(S_2)_m^j\right)\end{bmatrix}.$$

Solving the system (40), we get

$$V^{j+1}=\left[B_2-A_2A_1^{-1}B_1\right]^{-1}\left[A_2A_1^{-1}C_1+C_2\right], \tag{41a}$$

$$U^{j+1}=A_1^{-1}\left[B_1V^{j+1}+C_1\right]. \tag{41b}$$

4.2 | Numerical approximation via NUTS

Using the approximation given by Equation 19, along with eq. (1.5) in Equations 28 and 30, and using Equation 36, we get the following system:

$$\bar{A}_1U^{j+1}-\bar{B}_1V^{j+1}=\bar{C}_1, \tag{42a}$$

$$-\bar{A}_2U^{j+1}+\bar{B}_2V^{j+1}=\bar{C}_2, \tag{42b}$$

with

$$\bar{A}_1=A-\frac{h^2}{k_1}\left[2c_{j+1}^{j+1}B+2\alpha_3(BU)^j+\alpha_5(BV)^j+2\alpha_6(BUV)^j+\alpha_7\left(BV^2\right)^j\right],$$

$$\bar{B}_1=\frac{h^2}{k_1}\left[\alpha_2B+2\alpha_4(BV)^j+\alpha_5(BU)^j+\alpha_6\left(BU^2\right)^j+2\alpha_7(BUV)^j\right],$$

$$\bar{C}_1=\frac{h^2}{k_1}\Big[(\alpha_2B+\alpha_6\left(BU^2\right)^jV^j+\left(\alpha_1B-2c_{j+1}^{j+1}B-\alpha_7\left(BV^2\right)^j\right)U^j+2B\sum_{k=1}^{j+1}c_k^\alpha\left(U^k-U^{k-1}\right)+2\alpha_0BO$$
$$-AU^j+D\Big],\ \bar{A}_2=\frac{h^2}{k_2}\left[\beta_1B+2\beta_3(BU)^j+\beta_5(BV)^j+2\beta_6(BUV)^j+\beta_7\left(BV^2\right)^j\right],$$

$$\bar{B}_2=A-\frac{h^2}{k_2}\left[2c_{j+1}^{j+1}B+2\beta_2B+2\beta_4(BV)^j+\beta_5(BU)^j+\beta_6\left(BU^2\right)^j+2\beta_7(BUV)^j\right],$$

$$\bar{C}_2=\frac{h^2}{k_2}\left[\left(\beta_2B+\beta_6\left(BU^2\right)^j-2c_{j+1}^{j+1}\right)V^j+\left(\beta_1B-\beta_7\left(BV^2\right)^j\right)U^j+2B\sum_{k=1}^{j+1}c_k^\alpha\left(V^k-V^{k-1}\right)+2\beta_0BO-AV^j+E\right],$$

where $(BU)^j$,$(BV)^j$,$(BUV)^j$,$(BV^2)^j$,and $(BU^2)^j$ are tridiagonal matrices defined as follows.

$$(B\Omega)^j = \begin{cases} b_0\left(\Omega_i^j\right), & i=k, \\ b_0\left(\Omega_{i-1}^j\right), & i-k=1, \\ b_0\left(\Omega_{i+1}^j\right), & i-k=-1, \\ 0, & \text{otherwise}, \end{cases} \quad \Omega\in\{u,v,uv,u^2,v^2\} \text{ and } i,k=1,2,...,m-1.$$

O is ones, $m-1$ vector matrix, D and E are $(m-1)\times N$ zero matrices except for the elements in the first and last rows where

$$\begin{aligned} D(l,j) = &-\left(h_l^{j+1}+h_l^j\right)+\left(\frac{b_1h^2}{k_1}\right.\left[2c_{j+1}^{j+1}\left(h_l^{j+1}-h_l^j\right)+2\sum_{k=1}^{j}c_k^{j+1}\left(h_l^{j+1}-h_l^j\right)\right. \\ &+h_l^{j+1}\left(\alpha_1+2\alpha_3h_l^j+\alpha_5g_l^j+2\alpha_6h_l^jg_l^j+\alpha_7\left(g_l^j\right)^2\right)+g_l^{j+1}\left(\alpha_2+2\alpha_4g_l^j+\alpha_5h_l^j+2\alpha_6(h_l^j)^2+2\alpha_7g_l^jh_l^j\right) \\ &\left.\left.+\left(2\alpha_0+\alpha_1h_l^j+\alpha_2g_l^j+\alpha_6(h_l^j)^2g_l^j-\alpha_7\left(g_l^j\right)^2\right)h_l^j\right)\right], \end{aligned}$$

$$\begin{aligned} E(l,j) = &-\left(g_l^{j+1}+g_l^j\right)+\left(\frac{b_1h^2}{k_2}2c_{j+1}^{j+1}\left(g_l^{j+1}-g_l^j\right)+2\sum_{k=1}^{j}c_k^{j+1}\left(g_l^{j+1}-g_l^j\right)\right. \\ &+h_l^{j+1}\left(\beta_1+2\beta_3h_l^j+\beta_5g_l^j+2\beta_6h_l^jg_l^j+\beta_7\left(g_l^j\right)^2\right)+g_l^{j+1}\left(\beta_2+2\beta_4g_l^j+\beta_5h_l^j+2\beta_6(h_l^j)^2\right. \\ &\left.\left.+2\beta_7g_l^jh_l^j\right)+\left(2\beta_0+\beta_1h_l^j+\beta_2g_l^j+\beta_6(h_l^j)^2g_l^j-\beta_7\left(g_l^j\right)^2\right)h_l^j\right)., l=1,2,\ h_l^j=h_l(t_j), g_l^j=g_l(t_j), l=1,2, j=2,1,...,N. \end{aligned}$$

Solving the system (42), we get

$$V^{j+1}=\left[\bar{B}_2-\bar{A}_2\bar{A}_1^{-1}\bar{B}_1\right]^{-1}\left[\bar{A}_2\bar{A}_1^{-1}\bar{C}_1+\bar{C}_2\right], \tag{43a}$$

$$U^{j+1}=\bar{A}_1^{-1}\left[\bar{B}_1V^{j+1}+\bar{C}_1\right]. \tag{43b}$$

5 | THEORETICAL ANALYSIS

To study the theoretical analysis of the proposed technique, we let

$$u_h=\{u\mid u=(u_0,u_1,...,u_m)|u_0=u_m=0\}, \text{and } v_h=\{v\mid v=(v_0,v_1,...,v_m)|v_0=v_m=0\}$$

$\delta_x u_{i-\frac{1}{2}}=\frac{1}{h}(u_i-u_{i-1}), \delta_x v_{i-\frac{1}{2}}=\frac{1}{h}(v_i-v_{i-1})$, $\delta_x^2u_i=\frac{1}{h}\left(\delta_x u_{i+\frac{1}{2}}-\delta_x u_{i-\frac{1}{2}}\right)$, and $\delta_x^2v_i=\frac{1}{h}\left(\delta_x v_{i+\frac{1}{2}}-\delta_x v_{i-\frac{1}{2}}\right)$. Also, we introduce the following operator.

$$\mathcal{H}_hu_i=h^2(b_1u_{i+1}+b_0u_i+b_1u_{i-1}), \text{and } \delta_x^2u_i=u_{i+1}+au_i+u_{i-1}.$$

Lemma 5.1. Let $\eta(x)\in C^8[x_{i-1}, x_{i+1}]$, then

$$h^2\left(b_1\eta_{i+1}''+b_0\eta_i''+b_1\eta_{i-1}''\right)=\eta_{i+1}+a\,\eta_i+\eta_{i-1}+(lte_P)_i, \text{where}$$

$$\left(\mathrm{lte}_{\mathrm{P}}^{\mathrm{x}}\right)_{\mathrm{i}}=\begin{cases}\mathrm{h}^{6}\emptyset_{-1}(\mathrm{Z})\mathrm{D}^{6}\eta_{\mathrm{i}}+\mathrm{O}\left(\mathrm{h}^{8}\right),\mathrm{P}=-1,\\ \mathrm{h}^{6}\emptyset_{0}(\mathrm{Z})\mathrm{D}^{4}(\mathrm{D}^{2}-\mu_{0})\eta_{\mathrm{i}}+\mathrm{O}\left(\mathrm{h}^{8}\right),\mathrm{P}=0,\\ \mathrm{h}^{6}\emptyset_{1}(\mathrm{Z})\mathrm{D}^{2}(\mathrm{D}^{2}-\mu_{0})(\mathrm{D}^{2}-\mu_{1})\eta_{\mathrm{i}}+\mathrm{O}\left(\mathrm{h}^{8}\right),\mathrm{P}=1,\\ \mathrm{h}^{6}\emptyset_{2}(\mathrm{Z})(\mathrm{D}^{2}-\mu_{0})(\mathrm{D}^{2}-\mu_{1})(\mathrm{D}^{2}-\mu_{2})\eta_{\mathrm{i}}+\mathrm{O}\left(\mathrm{h}^{8}\right),\mathrm{P}=2,\end{cases}$$

where $\emptyset_P(Z_0,Z_1,...,Z_P)=-\frac{1}{240}+O(Z_0,Z_1,...,Z_P)$.

Applying Lemma 2.4 to our problem (1a,1b), we have

$$\sum_{k=1}^{j}c_k^j\left(u_i^k-u_i^{k-1}\right)=K_1D_{xx}u_i^j-f_{1i}^j+(lte^t)_i^j,\ \sum_{k=1}^{j}c_k^j\left(v_i^k-v_i^{k-1}\right)=K_2D_{xx}v_i^j-f_{2i}^j+(lte^t)_i^j. \tag{44}$$

Once we apply the operator $\mathcal{H}_h$ on Equation 44, one has

$$\mathcal{H}_h\sum_{k=1}^{j}c_k^j\left(u_i^k-u_i^{k-1}\right)=\mathcal{H}_hK_1D_{xx}u_i^j-\mathcal{H}_hf_{1i}^j+\mathcal{H}_h(lte^t)_i^j, \tag{45a}$$

$$\mathcal{H}_h\sum_{k=1}^{j}c_k^j\left(v_i^k-v_i^{k-1}\right)=\mathcal{H}_hK_2D_{xx}v_i^j-\mathcal{H}_hf_{2i}^j+\mathcal{H}_h(lte^t)_i^j. \tag{45b}$$

Using Lemma 5.1, we get

$$\mathcal{H}_hD_{xx}u_i^j=\delta_x^2u_i+\left(lte_P^x\right)_i^j,\mathcal{H}_hD_{xx}v_i^j=\delta_x^2v_i+\left(lte_P^x\right)_i^j. \tag{46}$$

From Equation 46 into Equation (45) leads to

$$\mathcal{H}_h\sum_{k=1}^{j}c_k^j\left(u_i^k-u_i^{k-1}\right)=K_1\delta_x^2u_i-\mathcal{H}_hf_{1i}^j+T_i^j, \tag{47a}$$

$$\mathcal{H}_h\sum_{k=1}^{j}c_k^j\left(v_i^k-v_i^{k-1}\right)=K_2\delta_x^2v_i-\mathcal{H}_hf_{2i}^j+T_i^j, \tag{47b}$$

where $T_i^j=K_1\left(lte_P^x\right)_i^j+\mathcal{H}_h(lte^t)_i^j$ and

$$\left|T_i^j\right|\le O\left(\tau^{3-\alpha}+h^6\right),P=0,1,2,\text{and}\left|T_i^j\right|\le O\left(\tau^{3-\alpha}+h^4\right),P=-1.$$

Eliminating the local truncation error, we obtain

$$\mathcal{H}_h\sum_{k=1}^{j}c_k^j\left(U_i^k-U_i^{k-1}\right)=K_1\delta_x^2U_i-\mathcal{H}_h\bar{f}_{1i}^j, \tag{48a}$$

$$\mathcal{H}_h\sum_{k=1}^{j}c_k^j\left(V_i^k-V_i^{k-1}\right)=K_2\delta_x^2V_i-\mathcal{H}_h\bar{f}_{2i}^j, \tag{48b}$$

$$U_0^j=h_1\left(t_j\right),U_m^j=h_2\left(t_j\right),V_0^j=g_1\left(t_j\right),V_m^j=g_2\left(t_j\right),\ 1\le j\le n, \tag{48c}$$

$$U_i^0=p_1(x_i),V_i^0=p_2(x_i),,\ 0\le i\le m. \tag{48d}$$

5.1 | Stability

Let $\bar{U}_i$ and $\bar{V}_i$ be two approximations of the system given by Equations 48a and 48b and define the round-off error

$$\sigma_i^j = U_i^j - \overline{U}_i^j, \bar{\sigma}_i^j = V_i^j - \overline{V}_i^j, 1 \le j \le n, 0 \le i \le m, \gamma_i^j = f_1\left(x_i, t_j, U_i^j, V_i^j\right) - \bar{f}_1\left(x_i, t_j, \overline{U}_i^j, V_i^j\right),\ \bar{\gamma}_i^j = f_2\left(x_i, t_j, U_i^j, V_i^j\right) - \bar{f}_2\left(x_i, t_j, U_i^j, \overline{V}_i^j\right), 1 \le j \le n, 0 \le i \le m.$$

Let $\sigma = \left(\sigma_0^j, \sigma_1^j, ..., \sigma_m^j\right)^t$, $\bar{\sigma} = \left(\bar{\sigma}_0^j, \bar{\sigma}_1^j, ..., \bar{\sigma}_m^j\right)^t$, $\left\|\sigma_i^j\right\|_\infty = \max_{0 \le i \le m} \left|\sigma_i^j\right| = \left|\sigma_{i^*}^j\right|$, and $\left\|\bar{\sigma}_i^j\right\|_\infty = \max_{0 \le i \le m} \left|\bar{\sigma}_i^j\right| = \left|\bar{\sigma}_{i^*}^j\right|$. Also, using the Lipschitz condition $\left|\gamma_i^j\right| \le L_u \left|\sigma_i^j\right|$ and $\left|\bar{\gamma}_i^j\right| \le L_v \left|\bar{\sigma}_i^j\right|$, and Equation (48), one has

$$\mathcal{H}_h c_j^j \left(U_i^j - U_i^{j-1}\right) + \mathcal{H}_h \sum_{k=1}^{j-1} c_k^j \left(U_i^k - U_i^{k-1}\right) = K_1 \delta_x^2 U_i - \mathcal{H}_h \bar{f}_{1i}^j, \tag{49a}$$

$$\mathcal{H}_h c_j^j \left(V_i^j - V_i^{j-1}\right) + \mathcal{H}_h \sum_{k=1}^{j-1} c_k^j \left(V_i^k - V_i^{k-1}\right) = K_1 \delta_x^2 V_i - \mathcal{H}_h \bar{f}_{2i}^j. \tag{49b}$$

Via a straightforward simplification, we have

$$b_1^u U_{i+1}^j + b_0^u U_i^j + b_1^u U_{i-1}^j = \frac{1}{c_j^j} \sum_{k=0}^{j-1} \left(c_{k+1}^j - c_k^j\right) \left(b_1 U_{i+1}^j + b_0 U_i^j + b_1 U_{i-1}^j\right), \tag{50a}$$

$$b_1^v V_{i+1}^j + b_0^v V_i^j + b_1^v V_{i-1}^j = \frac{1}{c_j^j} \sum_{k=0}^{j-1} \left(c_{k+1}^j - c_k^j\right) \left(b_1 V_{i+1}^j + b_0 V_i^j + b_1 V_{i-1}^j\right), \tag{50b}$$

where $b_1^u = b_1 - \frac{K_1}{c_j^j} - \frac{L_u}{c_j^j}, b_0^u = b_1 - \frac{K_1 a_0}{c_j^j} - \frac{L_u}{c_j^j}$, $b_1^v = b_1 - \frac{K_2}{c_j^j} - \frac{L_v}{c_j^j}, b_0^v = b_1 - \frac{K_2 a_0}{c_j^j} - \frac{L_v}{c_j^j}$.

Then the round-off system is given as

$$b_1^u \sigma_{i+1}^j + b_0^u \sigma_i^j + b_1^u \sigma_{i-1}^j = \frac{1}{c_j^j} \sum_{k=0}^{j-1} \left(c_{k+1}^j - c_k^j\right) \left(b_1 \sigma_{i+1}^k + b_0 \sigma_i^k + b_1 \sigma_{i-1}^k\right), \tag{51a}$$

$$b_1^v \bar{\sigma}_{i+1}^j + b_0^v \bar{\sigma}_i^j + b_1^v \bar{\sigma}_{i-1}^j = \frac{1}{c_j^j} \sum_{k=0}^{j-1} \left(c_{k+1}^j - c_k^j\right) \left(b_1 \bar{\sigma}_{i+1}^k + b_0 \bar{\sigma}_i^k + b_1 \bar{\sigma}_{i-1}^k\right). \tag{51b}$$

One can write the above system as

$$L_1^u \sigma_i^j = L_2^u \sigma_i^{j-1},\ L_1^v \bar{\sigma}_i^j = L_2^u \bar{\sigma}_i^{j-1}, \tag{52}$$

where

$$L_1^u \sigma_i^j = b_1^u \sigma_{i+1}^j + b_0^u \sigma_i^j + b_1^u \sigma_{i-1}^j, L_2^u \sigma_i^j = \frac{1}{c_j^j} \sum_{k=0}^{j-1} \left(c_{k+1}^j - c_k^j\right) \left(b_1 \sigma_{i+1}^k + b_0 \sigma_i^k + b_1 \sigma_{i-1}^k\right), \tag{53a}$$

$$L_1^v \bar{\sigma}_i^j = b_1^v \bar{\sigma}_{i+1}^j + b_0^v \bar{\sigma}_i^j + b_1^v \bar{\sigma}_{i-1}^j, L_2^u \bar{\sigma}_i^j = \frac{1}{c_j^j} \sum_{k=0}^{j-1} \left(c_{k+1}^j - c_k^j\right) \left(b_1 \bar{\sigma}_{i+1}^k + b_0 \bar{\sigma}_i^k + b_1 \bar{\sigma}_{i-1}^k\right). \tag{53b}$$

From Equations 53a and 53b, we have

$$\left|L_2^u\,\sigma_i^{j-1}\right| = \left|\frac{1}{c_j^j}\sum_{k=0}^{j-1}\left(c_{k+1}^j - c_k^j\right)\left(b_1\sigma_{i+1}^k + b_0\sigma_i^k + b_1\sigma_{i-1}^k\right)\right|,$$

$$\left|\sigma_i^{j-1}\right| = \max_{0\le k\le j-1}\left|\sigma_i^k\right|, c_0^j = 0, c_j^j > 0, \left|\sum_{k=0}^{j-1}\left(c_{k+1}^j - c_k^j\right)\right| = c_j^j.$$

$$\left|L_2^u\,\sigma_i^{j-1}\right| \le \left|b_1\sigma_{i+1}^{j-1}\right| + \left|b_0\sigma_i^{j-1}\right| + \left|b_1\sigma_{i-1}^{j-1}\right| \le (2b_1 + b_0)\left|\sigma_i^{j-1}\right|,$$

and

$$\left\|\sigma^j\right\|_\infty = \left|\sigma_i^j\right| = \left|b_1^u\,\sigma_{i+1}^j + b_0^u\sigma_i^j + b_1^u\sigma_{i-1}^j\right| = \left|L_1^u\,\sigma_i^j\right| = \left|L_2^u\,\sigma_i^{j-1}\right| \le (2b_1 + b_0)\left|\sigma_i^{j-1}\right| = \left\|\sigma^{j-1}\right\|_\infty.$$

We have $\|\sigma^j\|_\infty \le \|\sigma^0\|_\infty, 1 \le j \le n$; similarly, we have $\|\bar{\sigma}^j\|_\infty \le \|\bar{\sigma}^0\|_\infty, 1 \le j \le n$.

We brief the above results as follows.

Theorem 5.1. The MPEF system (48) is unconditionally stable.

5.2 | Convergence

To discuss the convergence of the scheme (48), let

$e_i^j = \mathrm{u}_i^j - U_i^j$, $\bar{e}_i^j = \mathrm{v}_i^j - V_i^j, 1 \le j \le n, 0 \le i \le m$, $\varepsilon_i^j = f_1\left(x_i, t_j, u_i^j, v_i^j\right) - \bar{f}_1\left(x_i, t_j, U_i^j, v_i^j\right)$,

$$\bar{\varepsilon}_i^j = f_2\left(x_i, t_j, u_i^j, v_i^j\right) - \bar{f}_2\left(x_i, t_j, u_i^j, V_i^j\right), 1 \le j \le n, 0 \le i \le m.$$

Using Equations (47) and (48), we have

$$L_1^u\,e_i^j = L_2^u\,e_i^{j-1} + T_i^j,\ L_1^v\varepsilon_i^j = L_2^u\,\varepsilon_i^{j-1} + T_i^j, \tag{54a}$$

$$e_0^j = e_m^j = \varepsilon_0^j = \varepsilon_m^j = 0,\ 1 \le j \le n, \tag{54b}$$

$$e_i^0 = \varepsilon_i^0,\ 0 \le i \le m. \tag{54c}$$

Define $\|e^j\|_\infty = \max_{0\le i\le m}\left|e_i^j\right| = \left|e_{i^*}^j\right|$ and $\|\varepsilon^j\|_\infty = \max_{0\le i\le m}\left|\varepsilon_i^j\right| = \left|\varepsilon_{i^*}^j\right|$, then one can obtain

$$\left\|e^j\right\|_\infty = \left|e_i^j\right| = \left|L_2^u\,e_i^{j-1} + T_i^j\right| \le \left|L_2^u\,e_i^{j-1}\right| + \left|T_i^j\right| \le \left\|e^{j-1}\right\|_\infty + \left\|T_i^j\right\|_\infty \le \left\|e^0\right\|_\infty + \left\|T_i^j\right\|_\infty \le \left\|T_i^j\right\|_\infty,$$

where $\|e^0\|_\infty = 0$ and $\left\|T_i^j\right\|_\infty = \max_{\mathrm{i,j}}\left|T_i^j\right|$.

Similarly, we have $\|\varepsilon^j\|_\infty \le \|\varepsilon^0\|_\infty + \left\|T_i^j\right\|_\infty \le \left\|T_i^j\right\|_\infty$, $\|\varepsilon^0\|_\infty = 0$. We can list all the above results as follows.

Theorem 5.2. Let $\left\{u(x_i,t_j)\right\}, \left\{u_i^j\right\}, \left\{v(x_i,t_j)\right\}$, and $\left\{v_i^j\right\}$, are solutions to the system (1a,1b) and the MPEF scheme (48) then

$$\left\|e^j\right\|_\infty \le \begin{cases} O\left(\tau^{3-\alpha}+h^6\right), P=0,1,2, \\ O\left(\tau^{3-\alpha}+h^4\right), P=-1, \end{cases} \text{and } \left\|\varepsilon^j\right\|_\infty \le \begin{cases} O\left(\tau^{3-\alpha}+h^6\right), P=0,1,2, \\ O\left(\tau^{3-\alpha}+h^4\right), P=-1, \end{cases} 1 \le j \le n.$$

6 | NUMERICAL EXAMPLES

In this section, the MPEF methods are verified by various test problems to reveal the accuracy of the developed techniques. The mean absolute error is $\text{MAE} = \frac{\sum_{j=0}^{n}\sum_{i=0}^{m} E_{i,j}}{(n+1)(m+1)}$, where $E^u = \left\|u(x_i,t_j) - u_i^j\right\|_\infty, E^v = \left\|v(x_i,t_j) - v_i^j\right\|_\infty$, and $\|.\|_\infty$ is the infinite norm.

6.1 | Example 1

Consider the time fractional reaction–diffusion system,[21,62]

$$D_t^\alpha u = D_x^2 u - 0.1u + v,\ 0 < \alpha \le 1, \tag{55a}$$

TABLE 1 The absolute errors for $P = -1, T = 10, m = 64$, and $\alpha = 1$ and different values of τ

	E^u			E^v		
x	$\tau = 0.1$	$\tau = 0.01$	$\tau = 0.001$	$\tau = 0.1$	$\tau = 0.01$	$\tau = 0.001$
0.1π	9.1752 e-6	5.8442154 e-8	5.7621094e-9	3.8450 e-7	3.5470 e-9	3.49851 e-10
0.2π	1. 0489 e-6	8.6928334 e-8	8.5721262 e-9	6.2562 e-8	5.2761 e-9	5.20464 e-10
0.3π	9.4439 e-7	8.2384967 e-8	8.1249712e-9	5.7131 e-8	5.0003 e-9	4.93315 e-10
0.4π	5.8427 e-7	5.1015438 e-8	5.0316016 e-9	3.5348 e-8	3.0964 e-9	3.05498 e-10

TABLE 2 The absolute errors for $P = -1, T = 10, m = 64$, and $\alpha = 1, \tau = 0.01$ for different values of $\psi(\tau)$

	E^u				E^v			
x	$\psi(\tau) = \sin\tau$	$\psi(\tau) = 1 - e^{-\tau}$	$\psi(\tau) = \tanh\tau$	$\psi(\tau) = \tau$	$\psi(\tau) = \sin\tau$	$\psi(\tau) = 1 - e^{-\tau}$	$\psi(\tau) = \tanh\tau$	$\psi(\tau) = \tau$
0.1π	5.825e-8	2.710 e-9	5.800e-8	5.844 e-8	3.535e-9	7.060 e-11	3.523e-9	3.547e-9
0.2π	8.665e-8	4.030e-9	8.637e-8	6.928 e-8	5.258e-9	1.051e-10	5.241e-9	5.276e-9
0.3π	8.212e-8	3.823 e-9	8.186e-8	8.238e-8	4.984e-9	9.968 e-11	4.967e-9	5.000e-9
0.4π	5.080e-8	2.367 e-9	5.060 e-8	5.101e-8	3.086 e-9	6.173 e-11	3.076e-9	3.096e-9

	E^u			E^v		
x	μ_q	μ_q^m	$\mu_q^{m_2}$	μ_q,	μ_q^m	$\mu_q^{m_2}$
0.1π	2.9e-8	2e-8	2.8 e-8	1.7e-9	1.6e-9	1.7e-9
0.2π	4.3e-5	4.2e-5	4.3e-5	2.6e-5	2.5e-5	2.6e-5
0.3π	4.0e-5	4.1e-5	4.0e-5	2.4e-5	2.4e-5	2.4e-5
0.4π	2.5e-5	2.5e-5	2.5e-5	1.5e-5	1.5e-5	1.5e-5

TABLE 3 The absolute errors for P=0,$T = 10, m = 64, \alpha = 1, \tau = 0.01$, and $\psi(\tau) = \tau$, where μ_q^m is the average of μ_q, $q = 0,...,N$, and $\mu_q^{m_2}$ is the average of μ_0 and μ_N

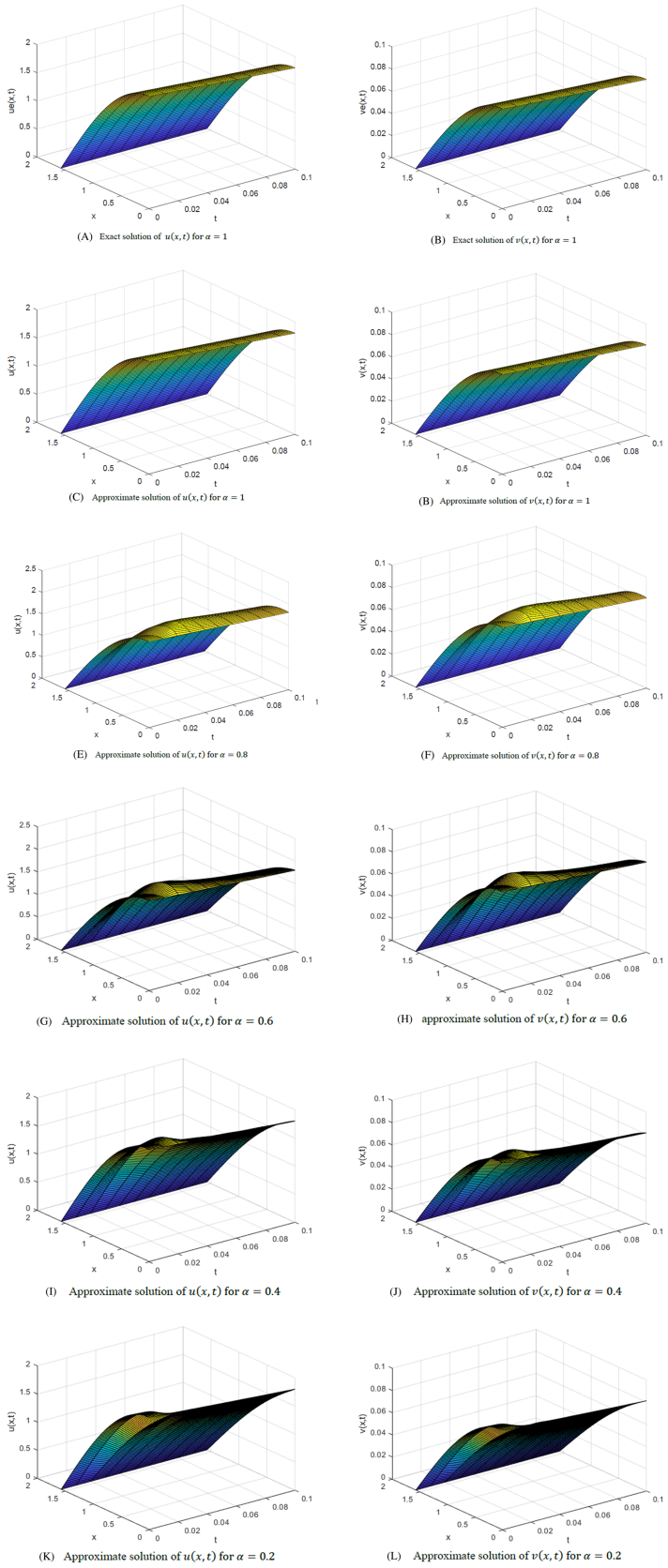

FIGURE 1 (A) Exact solution of $u(x,t)$ for $\alpha = 1$. (B) Exact solution of $v(x,t)$ for $\alpha = 1$. (C) Approximate solution of $u(x,t)$ for $\alpha = 1$. (D) Approximate solution of $v(x,t)$ for $\alpha = 1$. (E) Approximate solution of $u(x,t)$ for $\alpha = 0.8$. (F) Approximate solution of $v(x,t)$ for $\alpha = 0.8$. (G) Approximate solution of $u(x,t)$ for $\alpha = 0.6$. (H) Approximate solution of $v(x,t)$ for $\alpha = 0.6$. (I) Approximate solution of $u(x,t)$ for $\alpha = 0.4$. (J) Approximate solution of $v(x,t)$ for $\alpha = 0.4$. (K) Approximate solution of $u(x,t)$ for $\alpha = 0.2$. (L) Approximate solution of $v(x,t)$ for $\alpha = 0.2$ [Colour figure can be viewed at wileyonlinelibrary.com]

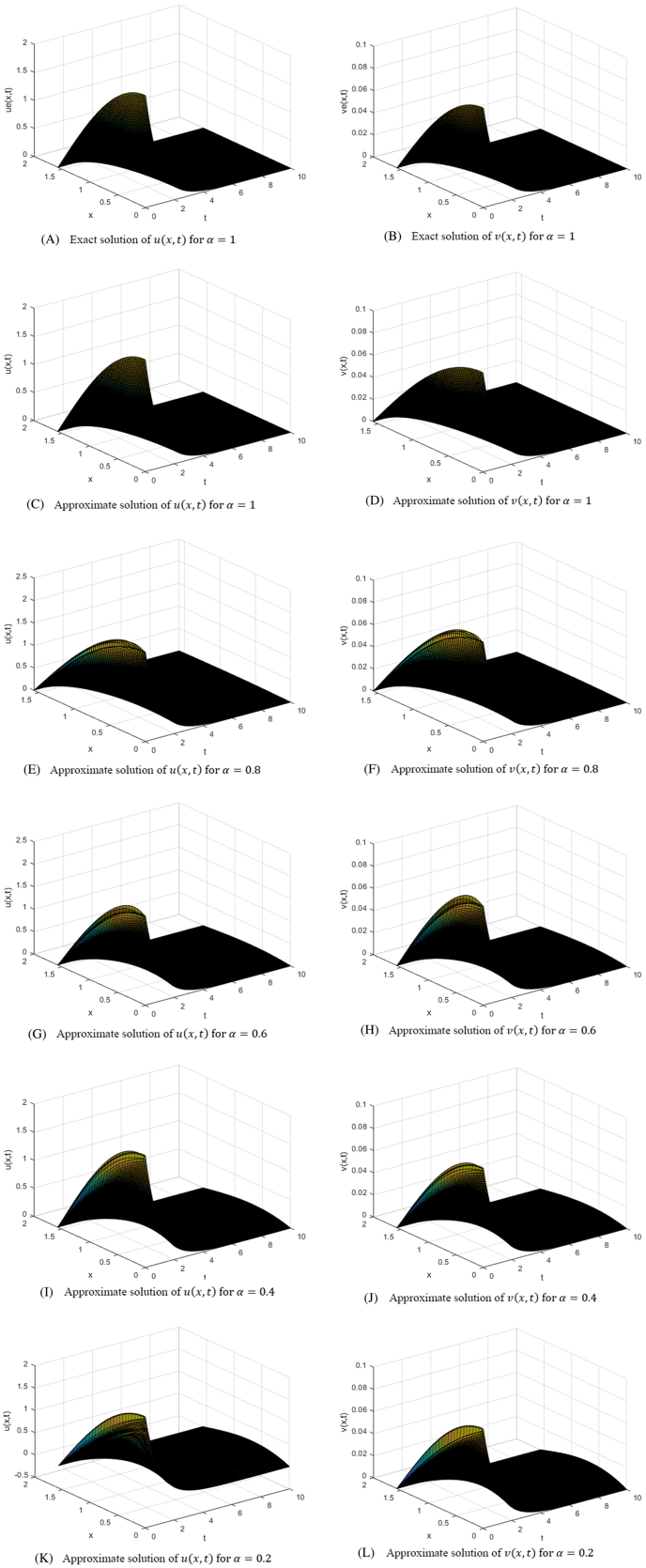

FIGURE 2 (A) Exact solution of $u(x,t)$ for $\alpha = 1$. (B) Exact solution of $v(x,t)$ for $\alpha = 1$. (C) Approximate solution of $u(x,t)$ for $\alpha = 1$. (D) Approximate solution of $v(x,t)$ for $\alpha = 1$. (E) Approximate solution of $u(x,t)$ for $\alpha = 0.8$. (F) Approximate solution of $v(x,t)$ for $\alpha = 0.8$. (G) Approximate solution of $u(x,t)$ for $\alpha = 0.6$. (H) Approximate solution of $v(x,t)$ for $\alpha = 0.6$. (I) Approximate solution of $u(x,t)$ for $\alpha = 0.4$. (J) Approximate solution of $v(x,t)$ for $\alpha = 0.4$. (K) Approximate solution of $u(x,t)$ for $\alpha = 0.2$. (L) Approximate solution of $v(x,t)$ for $\alpha = 0.2$ [Colour figure can be viewed at wileyonlinelibrary.com]

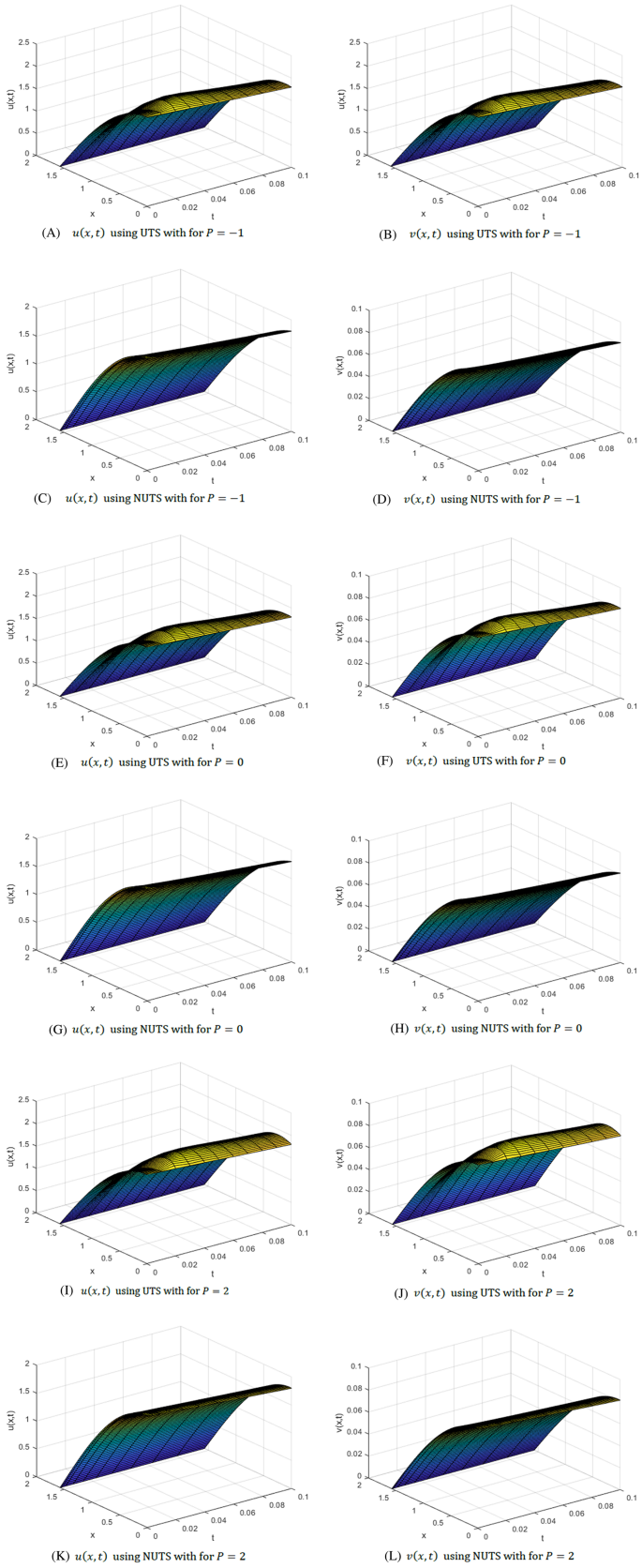

FIGURE 3 (A) $u(x,t)$ using UTS for $P=-1$. (B) $v(x,t)$ using UTS for $P=-1$. (C) $u(x,t)$ using NUTS for $P=-1$. (D) $v(x,t)$ using NUTS for $P=-1$. (E) $u(x,t)$ using UTS for $P=0$. (F) $v(x,t)$ using UTS for $P=0$. (G) $u(x,t)$ using NUTS for $P=0$. (H) $v(x,t)$ using NUTS for $P=0$. (I) $u(x,t)$ using UTS for $P=2$. (J) $v(x,t)$ using UTS for $P=2$. (K) $u(x,t)$ using NUTS for $P=2$. (L) $v(x,t)$ using NUTS for $P=2$ [Colour figure can be viewed at wileyonlinelibrary.com]

$$D_t^{\alpha} v = D_x^2 v - 0.01v, x \in \left[0, \frac{\pi}{2}\right], t \in [0, T],$$

with the boundary and initial conditions

$$u\left(\frac{\pi}{2}, t\right) = v\left(\frac{\pi}{2}, t\right) = u(0,t) - \left[e^{-1.1t} + e^{-1.01t}\right] = v(0,t) - 0.09e^{-1.01t} = 0, \tag{55b}$$

$u(x,0) = 2\cos x$, $v(x,0) = 0.09\cos x$, and the exact solution is

$$u(x,t) = \left[e^{-1.1t} + e^{-1.01t}\right]\cos x, v(x,t) = 0.09e^{-1.01t}\cos x.$$

This example is solved using the MPEF method $P = -1$ with time step $\tau = 0.001$, $\psi(\tau) = 1 - e^{-\tau}$ as the spatial and the nonstandard weighted shifted-Grünwald–Letnikov (NSWSGL) for temporal approximations. Table 1 shows the absolute errors for both $u(x,t)$, and $v(x,t)$. Also, Table 2 depicts the absolute errors for different choices of the function $\psi(\tau)$ and declares that the best choice is $\psi(\tau) = 1 - e^{-\tau}$. While Table 3 uses the method $P = 0$ to illustrate the effect of the solution when choosing the value of μ_q, $q = 0,...,N$. Also, Figures 1 and 2 give the solution plots of example 1 by the method $P = 0$ combined with NSWSGL with uniform time-stepping (UTS) for $T = 0.1$, and $T = 10$ for different values of α where $m = 64$, $\tau = 0.01$, $\psi(\tau) = 1 - e^{-\tau}$, and $\mu_q^{m_2}$. We can see that the solution plots have some oscillations near $t = 0$ for diverse values of α.

Finally, Figure 3 gives the solution plots of example 1 when $\alpha = 0.8$, $T = 0.1$, $n = 10$, $m = 64$, $\psi(\tau) = 1 - e^{-\tau}$, and $r = 2$ for different methods $P = -1,0$, and 2 with NSWSGL method with UTS and nonstandard high-order L1

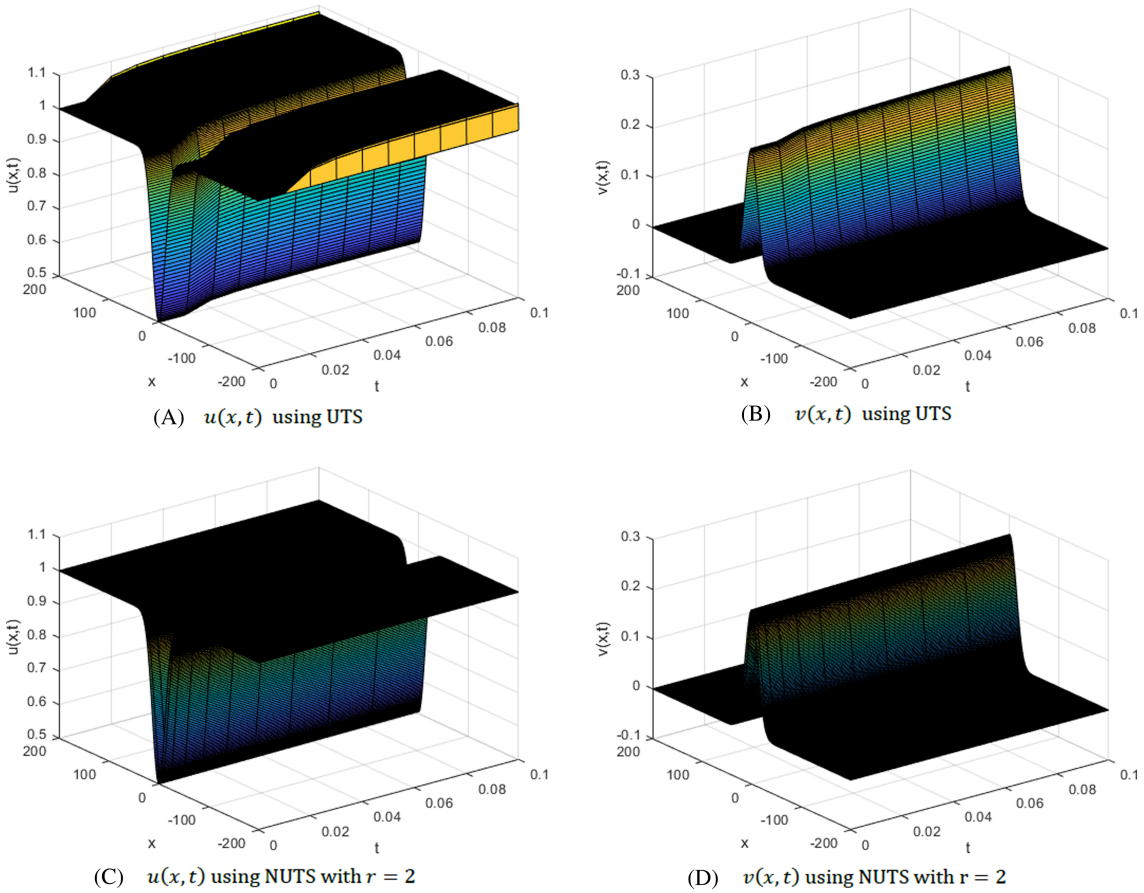

FIGURE 4 (A) $u(x,t)$ using UTS. (B) $v(x,t)$ using UTS. (C) $u(x,t)$ using NUTS with $r = 2$. (D) $v(x,t)$ using NUTS with $r = 2$ [Colour figure can be viewed at wileyonlinelibrary.com]

approximation with NUTS, respectively. We observe that all oscillations appear with NSWSGL-UTS have been eliminated when using nonstandard high order L1 approximation with NUTS as illustrated in Figure 3.

6.2 | Example 2

Consider the nonlinear time fractional reaction–diffusion system,

$$\mathrm{D}_t^{\alpha}u=\varepsilon_1 D_x^2u-u^2v+f(1-u),\ 0<\alpha\le 1, \tag{56a}$$

$$D_t^{\alpha}v=\varepsilon_2 D_x^2v+u^2v-(f+k)v, x\in[-L,L], t\in[0,T],$$

with the boundary and initial conditions

$$u(-L,t)=u(L,t)=1, v(-L,t)=v(L,t)=0, \tag{56b}$$

$$u(x,0)=1-0.5\sin^{100}\left(\sin\frac{\pi(x-L)}{2L}\right), v(x,0)=0.25\sin^{100}\left(\sin\frac{\pi(x-L)}{2L}\right),$$

where $\varepsilon_1=10^{-4}$, $\varepsilon_2=10^{-6}$, $f=0.024$, $k=0.06$, $L=200$.

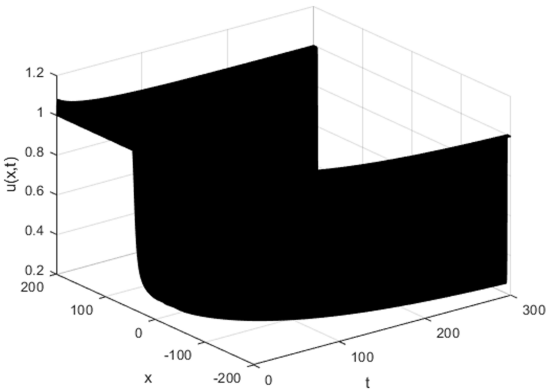

(A) The solution plot of $u(x,t)$ for example 2

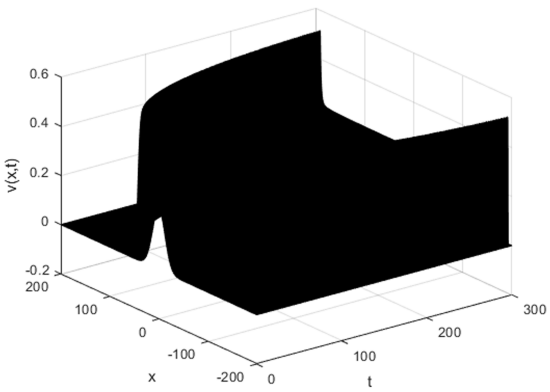

(B) The solution plot of $v(x,t)$ for example 2

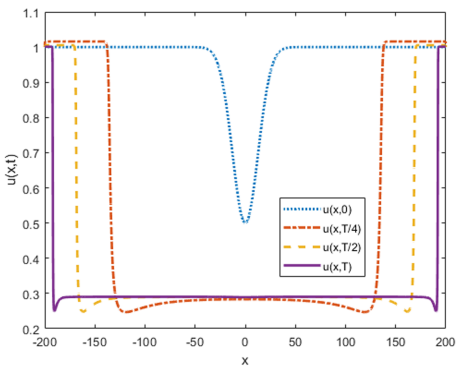

(C) The solution plot of $u(x,t)$ at the level times $T=0,\frac{T}{4},\frac{T}{2},T,T=300$

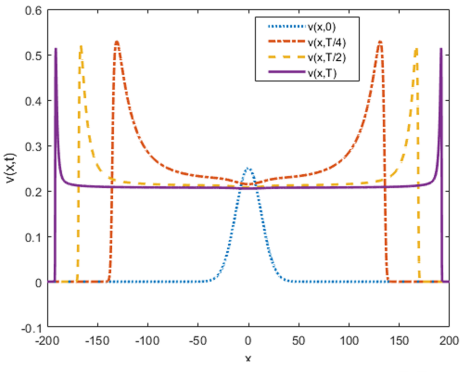

(D) The solution plot of $v(x,t)$ at the level times $T=0,\frac{T}{4},\frac{T}{2},T,T=300$

FIGURE 5 (A) The solution plot of $u(x,t)$ for example 2. (B) The solution plot of $v(x,t)$ for example 2. (C) The solution plot of $u(x,t)$ at the level times $T=0$, $T/4$, $T/2$, T, $T=300$. (D) The solution plot of $v(x,t)$ at the level times $T=0$, $T/4$, $T/2$, T, $T=300$ [Colour figure can be viewed at wileyonlinelibrary.com]

The numerical solution of example 3 for $\alpha = 0.9$, $T = 0.1$, $L = 200$, $n = 10$, $m = 4L$, $\psi(\tau) = \tau$, and $r = 2$ using the method $P = -1$ with the NSWSGL-UTS is presented in Figure 4A,B, and the nonstandard high-order L1 scheme with NUTS is shown in Figure 4C,D, respectively. Our new scheme illustrates the best performance when dealing with singularity behavior. Also, the solution graph of example 2 using NSWSGL-UTS for $T = 300$, $L = 200$, $n = 5T$, $m = 8L$, and $\psi(\tau) = \tau$ for the method $P = -1$ are shown in Figure 5 for different level times.

6.3 | Example 3: Gray–Scott: Pulse splitting[62]

Consider the nonlinear time-fractional reaction–diffusion system,

$$D_t^{\alpha} u = D_x^2 u - u^2 v + a(1-u),\ 0 < \alpha \leq 1, \tag{57a}$$

$$D_t^{\alpha} v = \varepsilon D_x^2 v + u^2 v - bv, x \in [-L, L], t \in [0, T],$$

with the boundary and initial conditions

$$u(-L,t) = u(L,t) = 1, v(-L,t) = v(L,t) = 0, \tag{57b}$$

$$u(x,0) = 1 - 0.5\sin^{100}\left(\sin\frac{\pi(x-L)}{2L}\right), v(x,0) = 0.25\sin^{100}\left(\sin\frac{\pi(x-L)}{2L}\right), -L < x < L$$

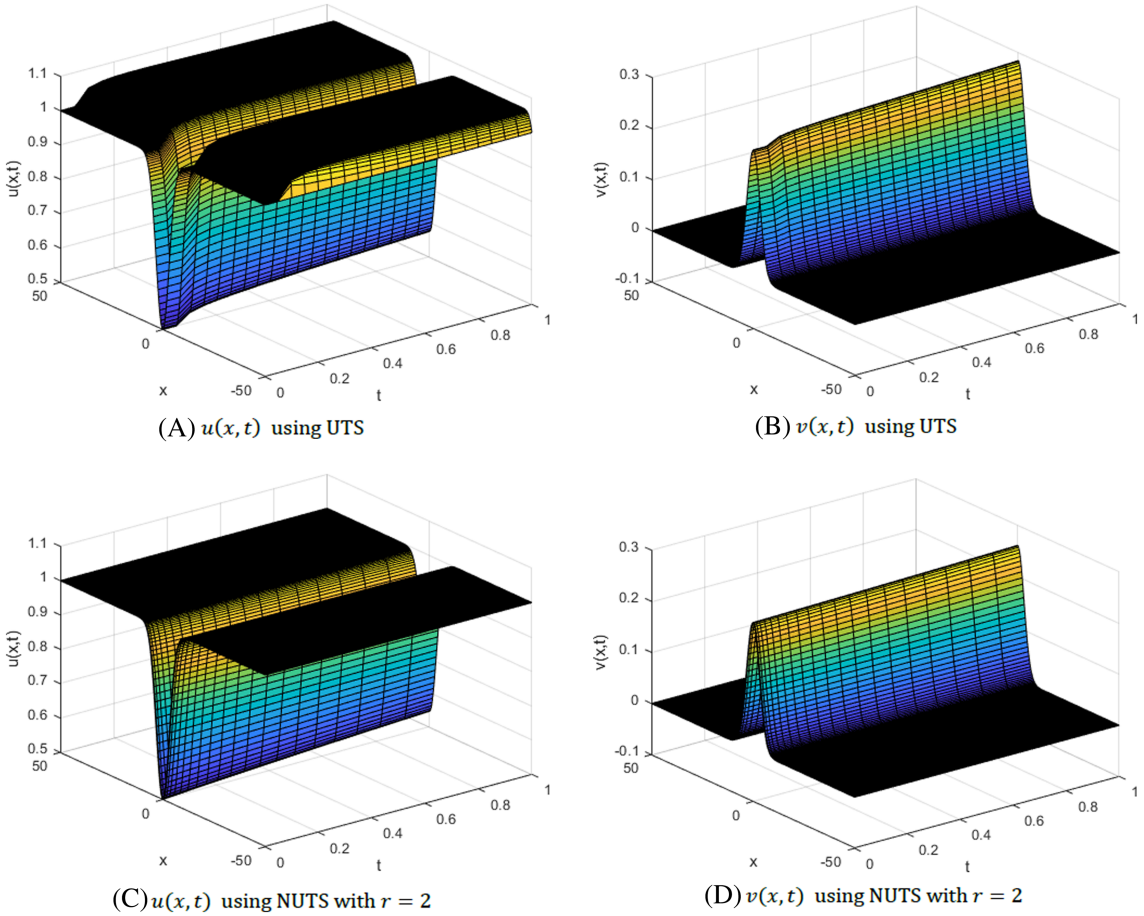

(A) $u(x,t)$ using UTS (B) $v(x,t)$ using UTS

(C) $u(x,t)$ using NUTS with $r = 2$ (D) $v(x,t)$ using NUTS with $r = 2$

FIGURE 6 (A) $u(x,t)$ using UTS. (B) $v(x,t)$ using UTS. (C) $u(x,t)$ using NUTS with $r = 2$. (D) $v(x,t)$ using NUTS with $r = 2$ [Colour figure can be viewed at wileyonlinelibrary.com]

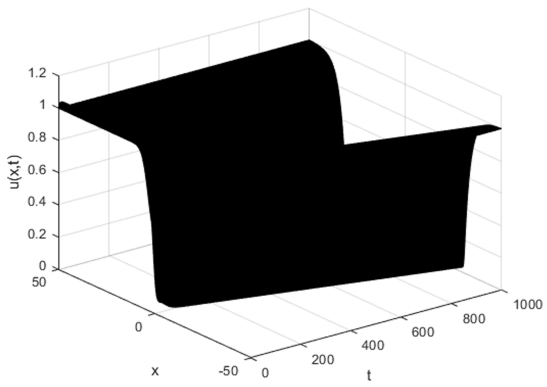

(A) The solution plot of $u(x,t)$ for example 3

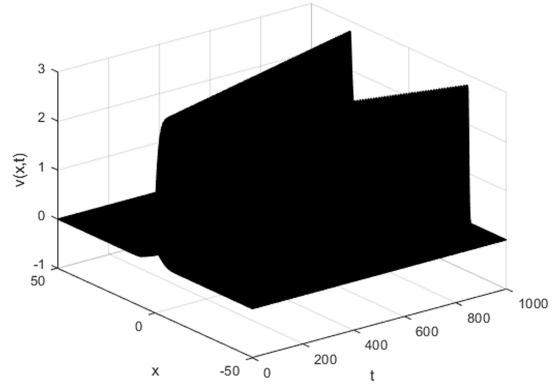

(B) The solution plot of $v(x,t)$ for example 3

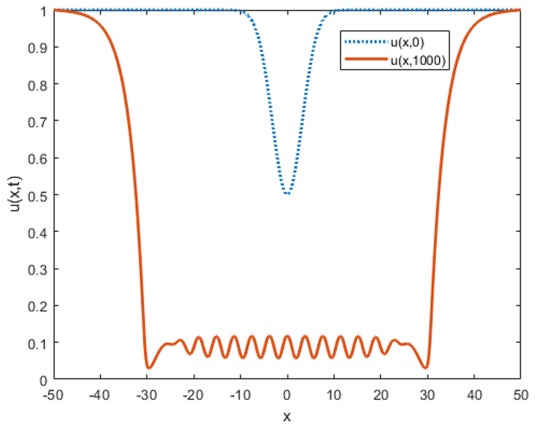

(C) The solution plot of $u(x,t)$ at the level times $T = 0,1000$

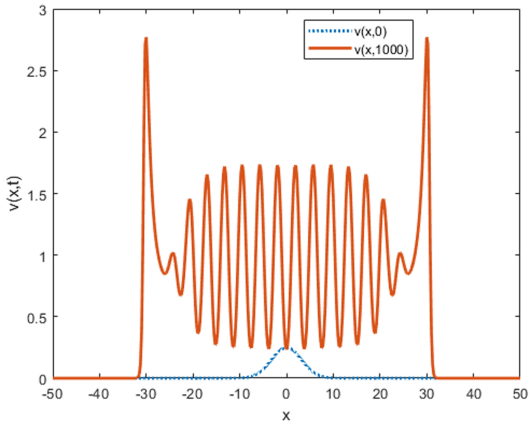

(D) The solution plot of $v(x,t)$ at the level times $T = 0,1000$

FIGURE 7 (A) The solution plot of $u(x,t)$ for example 3. (B) The solution plot of $v(x,t)$ for example 3. (C) The solution plot of $u(x,t)$ at the level times $T = 0$, 1000. (D) The solution plot of $v(x,t)$ at the level times $T = 0$, 1000 [Colour figure can be viewed at wileyonlinelibrary.com]

where $\varepsilon = 10^{-2}$,$L = 50$.

The numerical solution of example 3 for $\alpha = 0.9$, $T = 1$, $L = 50$, $n = 20$T, $m = 8L$, $\psi(\tau) = 1 - e^{-\tau}$, and $r = 2$ using the method $P = -1$ with the NSWSGL-UTS are presented in Figure 6A,B, and the nonstandard high-order L1 scheme with NUTS is shown in Figure 6C,D, respectively. Our new scheme illustrates the best performance when dealing with singularity behavior. Also, Figure 7A–D gives the solution graph of example 3 using NSWSGL-UTS when $T = 1000$.

7 | CONCLUSIONS

Two numerical schemes depending on the MPEF technique have been introduced for solving the time-fractional reaction–diffusion system. The first scheme based on the NSWSGL with uniform mesh provides some oscillations near $t = 0$ due to singularity behavior inherited in the system. The second approach depends on the nonstandard high-order L1 approximation for NUTS compensates these oscillations and increases the accuracy of the suggested method. Unconditional stability and convergence analysis have been derived. Some numerical illustrations have been applied to verify the theoretical studies.

ACKNOWLEDGEMENT

There are no funders to report for this submission.

CONFLICT OF INTEREST

This work does not have any conflicts of interest.

ORCID

Waheed K. Zahra https://orcid.org/0000-0002-6448-6877
Dumitru Baleanu https://orcid.org/0000-0002-0286-7244

REFERENCES

1. Onarcan AT, Adar N, Dag I. Trigonometric cubic B-spline collocation algorithm for numerical solutions of reaction–diffusion equation systems. *Comput Appl Math*. 2018;37(5):6848-6869. https://doi.org/10.1007/s40314-018-0713-4
2. Zahra WK, Hikal MM. Non standard finite difference method for solving variable order fractional optimal control problems. *J Vib Control*. 2017;23(6):948-958.
3. Maiti S, Shaw S, Shit GC. Caputo–Fabrizio fractional order model on MHD blood flow with heat and mass transfer through a porous vessel in the presence of thermal radiation. *Phys a Stat Mech its Appl*. 2020;540:1-17, 123149. https://doi.org/10.1016/j.physa.2019.123149
4. Sierociuk D, Dzielinski A, Sarwas G, Petras I, Podlubny I, Skovranek T. Modelling heat transfer in heterogeneous media using fractional calculus. *Philos Trans R Soc a Math Phys Eng Sci*. 2013;371(1990):1-10, 20120146. https://doi.org/10.1098/rsta.2012.0146
5. Qiao Y, Zhao J, Feng X. A compact integrated RBF method for time fractional convection–diffusion–reaction equations. *Comput Math Appl*. 2019;77(9):2263-2278. https://doi.org/10.1016/j.camwa.2018.12.017
6. Wazwaz AM. New travelling wave solutions to the Boussinesq and the Klein-Gordon equations. *Commun Nonlinear Sci Numer Simul*. 2008;13(5):889-901.
7. Wazwaz A-M. The tanh method: exact solutions of the sine-Gordon and the sinh-Gordon equations. *Appl Math Comput*. 2005;167(2):1196-1210. https://doi.org/10.1016/J.AMC.2004.08.005
8. Zahra WK, Nasr MA. Exponentially fitted methods for solving two-dimensional time fractional damped Klein–Gordon equation with nonlinear source term. *Commun Nonlinear Sci Numer Simul*. 2019;73:177-194. https://doi.org/10.1016/j.cnsns.2019.01.016
9. Kumar S, Kumar R, Cattani C, Samet B. Chaotic behaviour of fractional predator-prey dynamical system. *Chaos Solitons Fractals*. 2020;135:1-12, 109811. https://doi.org/10.1016/j.chaos.2020.109811
10. Ghanbari B, Kumar S, Kumar R. A study of behaviour for immune and tumor cells in immunogenetic tumour model with non-singular fractional derivative. *Chaos Solitons Fractals*. 2020;133:1-11. https://doi.org/10.1016/j.chaos.2020.109619
11. Kumar S, Kumar A, Samet B, Gómez-aguilar JF, Osman MS. Study of tumor and effector cells in fractional tumor-immune model for cancer treatment. *Chaos Solitons Fractals*. 2020;141:1-14, 110321. https://doi.org/10.1016/j.chaos.2020.110321
12. Chang A, Sun H, Zheng C, Lu B. A time fractional convection–diffusion equation to model gas transport through heterogeneous soil and gas reservoirs. *Physica a*. 2018;502:356-369. https://doi.org/10.1016/j.physa.2018.02.080
13. Kumar S, Mehdi M. New analytical method for gas dynamics equation arising in shock fronts. *Comput Phys Commun*. 2014;185(7):1947-1954. https://doi.org/10.1016/j.cpc.2014.03.025
14. Owolabi KM, Atangana A. Computational study of multi-species fractional reaction-diffusion system with ABC operator. *Chaos Solitons Fractals*. 2019;128:280-289. https://doi.org/10.1016/j.chaos.2019.07.050
15. Kumar S, Kumar R, Agarwal RP, Samet B. A study of fractional Lotka-Volterra population model using Haar wavelet and Adams-Bashforth-Moulton methods. *Math Method Appl Sci*. 2020;43:5564-5578. https://doi.org/10.1002/mma.6297
16. Kumar S. A new analytical modelling for fractional telegraph equation via Laplace transform. *App Math Model*. 2014;38(13):3154-3163. https://doi.org/10.1016/j.apm.2013.11.035
17. Atangana A, Qureshi S. Modeling attractors of chaotic dynamical systems with fractal–fractional operators. *Chaos Solitons Fractals*. 2019;123:320-337. https://doi.org/10.1016/j.chaos.2019.04.020
18. Owolabi KM. Numerical patterns in reaction – diffusion system with the Caputo and Atangana–Baleanu fractional derivatives. *Chaos Solitons Fractals*. 2018;115:160-169. https://doi.org/10.1016/j.chaos.2018.08.025
19. Lenzi EK, Neto RM, Tateishi AA, Lenzi MK, Ribeiro HV. Fractional diffusion equations coupled by reaction terms. *Physica a*. 2016;458:9-16. https://doi.org/10.1016/j.physa.2016.03.020
20. Wang T, Song F, Wang H, Karniadakis GE. Fractional Gray–Scott model: well-posedness, discretization, and simulations. *Comput Methods Appl Mech Eng*. 2019;347:1030-1049. https://doi.org/10.1016/j.cma.2019.01.002
21. Doelman A, Kaper TJ, Zegeling PA. Pattern formation in the one-dimensional Gray–Scott model. *Nonlinearity*. 1997;10(2):523-563. https://doi.org/10.1088/0951-7715/10/2/013
22. Owolabi KM. High-dimensional spatial patterns in fractional reaction-diffusion system arising in biology. *Chaos Solitons Fractals*. 2020;134:1-12, 109723. https://doi.org/10.1016/j.chaos.2020.109723
23. Owolabi KM, Hammouch Z. Spatiotemporal patterns in the Belousov–Zhabotinskii reaction systems with Atangana–Baleanu fractional order derivative. *Phys a Stat Mech its Appl*. 2019;523:1072-1090. https://doi.org/10.1016/j.physa.2019.04.017
24. Wang Y, Zhang R, Wang Z, Han Z. Turing pattern in the fractional Gierer–Meinhardt model. *Chin Phys B Vol*. 2019;28(5):1-7. https://doi.org/10.1088/1674-1056/28/5/050503
25. Mansouri D, Abdelmalek S, Bendoukha S. On the asymptotic stability of the time-fractional Lengyel – Epstein system. *Comput Math Appl*. 2019;78(5):1415-1430. https://doi.org/10.1016/j.camwa.2019.04.015

26. Khan MA, Atangana A. Modeling the dynamics of novel coronavirus (2019-nCov) with fractional derivative. *Alex Eng J*. 2020;59(4): 2379-2389. https://doi.org/10.1016/j.aej.2020.02.033
27. Kumar S, Nisar KS, Kumar R, Cattani C, Samet B. A new Rabotnov fractional-exponential function-based fractional derivative for diffusion equation under external force. *Math Methods Appl Sci*. 2020;43:4460-4471. https://doi.org/10.1002/mma.6208
28. Kumar S, Samet B. An analysis for heat equations arises in diffusion process using new Yang-Abdel-Aty-Cattani fractional operator. *Math Method Appl Sci*. 2020;43:6062-6080. https://doi.org/10.1002/mma.6347
29. Kumar S. Analytical solution of fractional Navier–Stokes equation by using modified Laplace decomposition method. *Ain Shams Eng J*. 2014;5(2):569-574. https://doi.org/10.1016/j.asej.2013.11.004
30. Kumar S, Kumar A, Baleanu D. Two analytical methods for time-fractional nonlinear coupled Boussinesq–Burger' s equations arise in propagation of shallow water waves. *Nonlinear Dyn*. 2016;85(2):699-715. https://doi.org/10.1007/s11071-016-2716-2
31. Doungmo EF, Kumar S, Mugisha SB. Similarities in a fifth-order evolution equation with and with no singular kernel. *Chaos Solitons Fractals*. 2020;130:24-26. https://doi.org/10.1016/j.chaos.2019.109467
32. Zahra WK, Nasr MA, Van Daele M. Exponentially fitted methods for solving time fractional nonlinear reaction–diffusion equation. *Appl Math Comput*. 2019;358:468-490. https://doi.org/10.1016/j.amc.2019.04.019
33. Vanden Berghe G, Van Daele M. Exponentially-fitted Numerov methods. *J Comput Appl Math*. 2007;200(1):140-153. https://doi.org/10.1016/j.cam.2005.12.022
34. Hollevoet D, Van Daele M, Vanden Berghe G. The optimal exponentially-fitted Numerov method for solving two-point boundary value problems. *J Comput Appl Math*. 2009;230(1):260-269. https://doi.org/10.1016/j.cam.2008.11.011
35. Ixaru LG. Operations on oscillatory functions. *Comput Phys Commun*. 1997;25(1):1-19. https://doi.org/10.1016/S0097-8485(00)00087-5
36. Mohebbi A, Abbaszadeh M, Dehghan M. High-order difference scheme for the solution of linear time fractional Klein–Gordon equations. *Numer Methods Partial Differ Equ*. 2014;30(4):1234-1253. https://doi.org/10.1002/num.21867
37. Dehghan M, Mohebbi A. High order implicit collocation method for the solution of two-dimensional linear hyperbolic equation. *Numer Methods Partial Differ Equ*. 2009;25(1):232-243.
38. Jin B, Lazarov R, Zhou Z. An analysis of the L1 scheme for the subdiffusion equation with nonsmooth data. *IMA J Numer Anal*. 2015; 36:197-221.
39. Zahra WK, Elkholy SM, Fahmy M. Rational spline-nonstandard finite difference scheme for the solution of time-fractional Swift–Hohenberg equation. *Appl Math Comput*. 2019;343:372-387. https://doi.org/10.1016/j.amc.2018.09.015
40. McLean W, Mustapha K. Time-stepping error bounds for fractional diffusion problems with non-smooth initial data. *J Comput Phys*. 2015;293:201-217.
41. Liao HL, Tang T, Zhou T. A second-order and nonuniform time-stepping maximum-principle preserving scheme for time-fractional Allen-Cahn equations. *J Comput Phys*. 2020;414:1-16, 109473. https://doi.org/10.1016/j.jcp.2020.109473
42. Soori Z, Aminataei A. A new approximation to Caputo-type fractional diffusion and advection equations on non-uniform meshes. *Appl Numer Math*. 2019;144:21-41. https://doi.org/10.1016/j.apnum.2019.05.014
43. Fazio R, Jannelli A. A finite difference method on non-uniform meshes for time-fractional advection – diffusion equations with a source term. *Appl Sci*. 2018;8(6):1-16. https://doi.org/10.3390/app8060960
44. Zhang Y, Sun Z, Liao H. Finite difference methods for the time fractional diffusion equation on non-uniform meshes. *J Comput Phys*. 2014;265:195-210. https://doi.org/10.1016/j.jcp.2014.02.008
45. Lin Y, Xu C. Finite difference/spectral approximations for the time-fractional diffusion equation. *J Comput Phys*. 2007;225(2):1533-1552. https://doi.org/10.1016/j.jcp.2007.02.001
46. Hou T, Tang T, Yang J. Numerical analysis of fully discretized Crank–Nicolson scheme for fractional-in-space Allen–Cahn equations. *J Sci Comput*. 2017;72(3):1214-1231. https://doi.org/10.1007/s10915-017-0396-9
47. Sales Teodoro G, Tenreiro Machado JA, Capelas de Oliveira E. A review of definitions of fractional derivatives and other operators. *J Comput Phys*. 2019;388:195-208. https://doi.org/10.1016/j.jcp.2019.03.008
48. Oldham KB, Spanier J. *The fractional calculus: theory and applications of differentiation and integration to arbitrary order*. New York and London: Academic Press; 1974:322.
49. Miller KS, Ross B. *An introduction to the fractional calculus and fractional differential equations*. New York: Wiley-Interscience; 1993:384.
50. Sousa E. How to approximate the fractional derivative of order $1 < \alpha \leq 2$. *Int J Bifurc Chaos*. 2012;22:1-13. https://doi.org/10.1142/S0218127412500757
51. Zahra WK, Daele MV. Discrete spline methods for solving two point fractional Bagley–Torvik equation. *Appl Math Comput*. 2017;296: 42-56. https://doi.org/10.1016/j.amc.2016.09.016
52. Gao GH, Sun HW, Sun ZZ. Some high-order difference schemes for the distributed-order differential equations. *J Comput Phys*. 2015; 298:337-359. https://doi.org/10.1016/j.jcp.2015.05.047
53. Zhou H, Tian W, Deng W. Quasi-compact finite difference schemes for space fractional diffusion equations. *J Sci Comput*. 2012;56(1): 45-66. https://doi.org/10.1007/s10915-012-9661-0
54. Mickens RE. *Nonstandard Finite Difference Models of Differential Equations*. Singapore: World Scientific Publishing Co Pte Ltd; 1994.
55. Zahra WK, Hikal MM. On fractional model of an HIV/AIDS with treatment and time delay. *Progr Fract Differ Appl*. 2016;2:55-66.
56. Ixaru LG, Vanden Berghe G. *Exponential Fitting*. New York: Springer-Verlag New York Inc.; 2004 https://doi.org/10.1007/978-1-4020-2100-8.

57. Coleman JP, Ixaru LG. Truncation errors in exponential fitting for oscillatory problems. *SIAM J Numer Anal*. 2006;44(4):1441-1465. https://doi.org/10.1137/050641752
58. Hollevoet D, Van Daele M, Vanden Berghe G. Exponentially fitted methods applied to fourth-order boundary value problems. *J Comput Appl Math*. 2011;235(18):5380-5393. https://doi.org/10.1016/j.cam.2011.05.049
59. Van Daele M, Hollevoet D, Vanden Berghe G. Multiparameter exponentially-fitted methods applied to second-order boundary value problems. *AIP Conf Proc*. 2009;1168:750-753. https://doi.org/10.1063/1.3241582
60. Rubin SG, Graves Jr RA. A cubic spline approximation for problems in fluid mechanics, NASA STI/recon tech. Rep. N. 75 (1975) R-436. http://ntrs.nasa.gov/archive/nasa/casi.ntrs.nasa.gov/19750025272.pdf.
61. Ouf WA, Zahra WK, El-Azab MS. Numerical simulation for the solution of nonlinear Jaulent-Miodek coupled equations using quartic B-spline. *Acta Univ Apulensis*. 2016;3:35-52. https://doi.org/10.17114/j.aua.2016.46.04
62. Korkmaz A, Ersoy O, Dag I. Motion of patterns modeled by the Gray-Scott autocatalysis system in one dimension, MATCH Commun. *Math Comput Chem*. 2017;77:507-526.

How to cite this article: Zahra WK, Hikal MM, Baleanu D. Numerical simulation for time-fractional nonlinear reaction–diffusion system on a uniform and nonuniform time stepping. *Math Meth Appl Sci*. 2021;44:5340–5364. https://doi.org/10.1002/mma.7114